NUREG/CR-2580
UCRL-15433
RD, RM

Structural Review of the Robert E. Ginna Nuclear Power Plant Under Combined Loads for the Systematic Evaluation Program

Manuscript Completed: December 1981
Date Published:

Prepared by
D. Wesley and H. Banon
Structural Mechanics Associates
P.O. 5133901

Lawrence Livermore National Laboratory
7000 East Avenue
Livermore, CA 94550

Prepared for
Office of Nuclear Regulatory Research
U.S. Nuclear Regulatory Commission
Washington, D.C. 20555
NRC FIN No. A-0436

ABSTRACT

An evaluation of the capacity of the Robert E. Ginna containment structure to withstand combined Loss-of-Coolant-Accident (LOCA) and seismic loads was conducted as part of the Systematic Evaluation Program (SEP). Seismic loads were developed by scaling the loads developed previously in the SEP program for the 0.2g peak ground acceleration SSE to 0.17g which is consistent with the site specific ground response spectra developed by Lawrence Livermore National Laboratory (LLNL). Thermal and pressure loads were developed from pressure and temperature transients developed by LLNL for the LOCA conditions.

An axisymmetric, multilayer shell of revolution analytical model was developed for the containment vessel. The model included the concrete vertical wall and dome and included the steel liner. Appropriate boundary conditions representing the shell-to-base-slab interface through neoprene pads were included. Since the base slab is founded on rock and the presence of the neoprene pads essentially isolates the base slab from the containment vessel, the base slab was not included in the model. No details, such as hatches or other penetrations, were evaluated in this phase of the SEP.

The analysis indicates that for the cylindrical portion of the vessel, liner and concrete stresses remain relatively low for the combined load condition and no damage is expected. In the vicinity of the base slab-containment wall interface, some localized yielding of the liner in the knuckle is predicted based on minimum code strength values.

Local liner buckling is expected in the uninsulated area of the dome in the event of a LOCA. The thermal gradient in the liner at the top of the insulation results in a correspondingly large stress gradient in the liner in this area. The resulting loads must be resisted by the concrete anchor studs in shear. Failure of some of these studs in pull out from the concrete under the insulation is expected, and failure of the liner integrity can conceivably occur in this region.

FOREWARD

The U.S. Nuclear Regulatory Commission (NRC) is conducting the Systematic Evaluation Program (SEP) which consists of a plant-by-plant limited reassessment of the safety of eleven operating nuclear reactors that received construction permits between 1956 and 1967. Because many safety criteria have changed since these plants were initially licensed, the purpose of the SEP is to develop a current documented basis for the safety of these older facilities.

For the Robert E. Ginna Nuclear Power Plant, seismic analyses for Safe Shutdown Earthquake (SSE) had been performed in a previous study for selected plant structures and components from generic groups of equipment, the results were reported in an earlier SEP report, NUREG/CR-1821. The SSE was considered to be the Extreme Environmental condition. In this study, the containment structure was selected to be further evaluated for the Abnormal/Extreme Environment.

The report reflects a collective effort on the part of the following persons:

Nelson, T. A., and Lo, T., (Lawrence Livermore National Laboratory), who provided project management support and reviewed the report.

Wesley, D. A., and Banon, H., (Structural Mechanics Associates), who conducted the structural reevaluation of the containment structure.

The authors wish to thank P. Y. Chen and S. Brown, technical monitors of this work at the NRC, for their continuing support.

0019G/mw

TABLE OF CONTENTS

LIST OF TABLES

LIST OF FIGURES

LIST OF FIGURES (Continued)

LIST OF FIGURES (Continued)

SUMMARY

An axisymmetric, multilayer shell of revolution analytical model was developed for the Ginna containment vessel. The model included the concrete vertical wall and dome and included the 3/8-inch steel liner. Appropriate boundary conditions representing the shell to base slab interface through neoprene pads were included. Since the base slab is founded on rock and the presence of the neoprene pads essentially isolates the base slab from the containment vessel, the base slab was not included in the model nor were the concrete internal structure or NSSS.

The loads included in this evaluation included the normal dead weight and operating conditions, peak pressure and thermal loads resulting from a Loss of Coolant Accident (LOCA), and the seismic response loads for the Safe Shutdown Earthquake (SSE). Pressure and temperature transients were developed by LLNL for Ginna, and the seismic loads were developed by scaling the loads developed in the SEP seismic program to 0.17g. Transient thermal gradients in the containment vessel were computed based on the inner surface steel liner temperature supplied by LLNL.

The analysis indicates that for the cylindrical portion of the vessel, liner and concrete stresses remain relatively low for the combined load condition and no damage is expected. Based on an uncracked analysis in the uninsulated hemispherical dome, high (approximately 6 ksi) thermal compressive stresses occur in approximately the inner 0.8 inch of concrete. However, a cracked section analysis of the containment shell in the dome shows that reinforcing steel and concrete stresses are below the code allowable stresses.

Due to the base slab-containment vessel wall connection detail, it is anticipated that most of the lateral seismic shear force will be carried by the liner knuckle. A maximum shear stress of approximately 21,000 psi is expected for the 32,000 psi minimum yield strength liner material. Since the code allowable yield strength in shear is 0.60 S_y or approximately 19,200 psi, yielding of the liner in the knuckle may possibly occur in a very localized area. Radial restraint to withstand the temperature and pressure loads at the base slab-containment vessel interface is provided by radial bars. The maximum tensile stress in these bars under the combined loads is approximately 54 ksi. The 130 ksi minimum yield strength of these bars provides a substantial margin of safety. The seismic overturning moment in combination with internal pressure is resisted by the dead weight of the vessel and the rock anchors. A factor of safety of approximately 1.0 exists for separation of the cylinder and base slab assuming 7 percent of critical damping in the seismic response of the structure. However, the liner knuckle is expected to have adequate flexibility to resist some uplift without failure.

Local liner buckling is expected in the uninsulated area due to the high liner temperature predicted in the event of a LOCA. The thermal gradient in the liner at the top of the insulation results in a correspondingly large stress gradient in the liner in this area. The resulting loads must be resisted by the concrete anchor studs in shear. Based on the assumption that the post-buckled load in the liner is equal to the critical load and assuming the thermal gradient in the liner from the uninsulated liner temperature to the insulated temperature occurs over a distance of two feet, the studs are expected to have inadequate capacity to resist the thermal loads, and pull out from the concrete is expected. Failure of the studs under the insulation is expected to progress part of the way down towards the first embedded channel depending on the post-buckled load as the buckled span increases in this region. Although the failure mode is expected to be pull out of the studs from the concrete, the integrity of the liner cannot be guaranteed.

Several options to correct this potential problem are apparent. One is to extend the insulation throughout the dome. A second is to remove the insulation in the dome to the spring line where the embedded channels provide a higher capacity anchorage system. Finally, some additional analysis to determine the post-buckled load in the liner and the thermal gradient in the liner in the area of the edge of the insulation could be conducted.

1. INTRODUCTION

As part of the Systematic Evaluation Program (SEP), Lawrence Livermore National Laboratory (LLNL) is conducting an evaluation of the capacity of a number of operating reactors subjected to combined seismic and Loss of Coolant Accident (LOCA) loads. This work is being performed for the U.S. Nuclear Regulatory Commission (NRC) and is a continuation of an evaluation previously conducted by LLNL to assess the seismic adequacy of the plants. This report describes the work conducted by Structural Mechanics Associates, Inc., in support of LLNL to determine the capacity of the Robert E. Ginna Nuclear Power Plant containment building to withstand combined seismic and LOCA load conditions. In this report, LOCA includes both primary loop loss-of-coolant-accident as well as secondary loop steam line break.

1.1 SCOPE OF EVALUATION

The depth of analysis and acceptance criteria for SEP plants are significantly different from those that would be required were the review being conducted in accordance with the current version of the Standard Review Plan. The scope of the SEP evaluation is to concentrate only on the overall behavior of the containment building to withstand the combined seismic and LOCA pressure and thermal loads and identify areas where additional effort is required. Therefore, numerous details such as personnel and equipment hatches as well as piping and electrical penetrations are not included. The containment shell is assumed to be adequately reinforced around the equipment hatch and other openings so that the effects of these openings on the overall shell response are assumed to be small. Neither are any jet impingement or pipe whip forces being considered during this phase of the SEP. Consequently, analytical techniques capable of describing the gross behavior of the structure to seismic, pressure, and thermal loads are considered adequate without the need to concentrate on local effects and details. The primary objective is to develop an overall assessment of the integrity of the liner to

withstand the combined loads. This requires a consideration of the response of the containment building but no evaluation of the internal structures is included.

In general, the current review is not based on demonstrating compliance with specific design codes or other current acceptance criteria. This has also been the approach used to date in conducting the seismic evaluation of the SEP plants (Reference 1). While capacity reduction factors (ϕ factors) and similar approaches are necessary in the design codes, the evaluation conducted for Ginna is based on unfactored loads. However, the original loads used in the Ginna design as obtained from the FSAR are also included for comparison, although the calculations used to develop the design loads were not reviewed nor were the design stress analyses available.

The load combinations investigated for the SEP include the deadweight, prestress, peak accident pressure and the thermal loads associated with the peak accident pressure, peak thermal loads and the pressure loads associated with the peak thermal loads, and the seismic loads resulting from the Safe Shutdown Earthquake (SSE). Other factored load combinations such as would be required for current licensing analyses were not considered. The SSE loads were developed for a 0.17g peak ground acceleration and the accident temperature and pressure loads were developed by LLNL.

2. STRUCTURE DESCRIPTION

The Ginna reactor containment building is a reinforced concrete cylinder with hemispherical dome. The structure has vertical prestressing tendons in the cylindrical wall which are anchored to bedrock. The structure is supported on a ring girder and two-foot thick base slab which are, in turn, founded on the bedrock. An additional nominal two-foot thick concrete fill covers the bottom liner plate, and the base slab is further stiffened by the ring girder under the cylindrical shell. The inside diameter of the cylinder is 105 feet and the cylindrical walls are 3'-6" thick. The reinforced concrete dome is 2'-6" thick. The overall height of the structure from the bottom of the base slab is 156 feet. The concrete internal structure is supported entirely on the base slab. No structural connections exist between the concrete internal structure and the containment shell, and radial gaps permit unrestrained relative motion between the two structures. Figure 2-1 shows the overall configuration of the reactor building including the internals and major NSSS equipment items. Figure 2-2 indicates the configuration of the containment vessel structure.

2.1 ROCK ANCHORS

The prestressed rock anchors provide the capacity for all vertical loads. These rock anchors are grouted into the sandstone bedrock rather than terminating in a tendon gallery beneath the base slab as is the more typical design practice. The cylindrical containment vessel is separated from the base slab by a neoprene pad. This detail is designed to prevent any shear transfer from the cylinder to the base slab.

The rock anchors are grouted in two stages into 6-inch diameter holes drilled into the sandstone to a depth of 26.5 feet. The capacity of the rock anchors was originally developed (Reference 2) assuming a 45^{o} breakout angle using the submerged weight of rock and the internal

vessel pressure, but taking no credit for tensile strength of the rock. The rock has an allowable bearing pressure of 35 tons per square foot and a recommended allowable lateral resistance of 25,000 psf.

2.2 PRESTRESSING SYSTEM

The vertical prestressing system uses the BBRV System with 90 wire tendons. The cold drawn wires are 1/4-inch in diameter with cold upset buttonheads 3/8-inch nominal diameter. The wires are fabricated to ASTM A-421-59T Type BA with a guaranteed ultimate tensile strength of 240,000 psi. The effective prestress in the tendons considering all losses is 60 percent of ultimate stress (144 ksi). The tendons are unbonded and pass through a bellows allowing up to 1/8-inch movement at the location of the cylinder wall-base slab junction as shown in Figure 2-3. The 90 wires are arranged in a hexagonal shaped cross section tendon at the lower end, with a maximum dimension across the vertices of approximately 5.08 inches, which passes through a 6-inch schedule 40 pipe sleeve. Thus, nearly one inch of clearance is available to allow relative motion between the containment vessel shell and the base slab before any shear loads are imposed on the tendons. The approximate outside diameter of the tendon at the upper end anchor is approximately 5-1/4 inches.

2.3 BASE SLAB-WALL CONNECTION

The detail of the containment structure cylinder junction with the base slab is also somewhat unique for Ginna. The concrete vertical wall rests on a series of neoprene pads as shown in Figure 2-3. The pads are approximately 1-5/8-inch thick constructed of two layers of 55 durameter hardness neoprene and three steel shims. The vertical tendons penetrate the pads but no reinforcing steel connects the containment vessel wall and base slab through the pads. Radial tension rods of high strength 1-3/8-inch diameter steel and the 3/8-inch thick liner provide the load transfer paths for radial and tangential shear, respectively. The radial bars have a minimum ultimate tensile strength of 145,000 psi and a yield strength of 130,000 psi and are spaced approximately 1 foot

1 inch on center at the centerline of the vertical wall. A sleeve provides clearance and hence allows relative motion between the base slab and wall resulting from neoprene pad deformation without imposing shear forces in the rods.

2.4 CONTAINMENT LINER

The 3/8-inch thick liner is fabricated from ASTM A442-60T Grade 60 steel plate with a minimum yield strength of 32,000 psi. The liner design at the base slab and vertical wall interface is in the form of a knuckle with a 10-inch radius. The stiffness of the knuckle was calculated assuming anchors at the tangent point for the vertical wall and 4-1/8 inches from the base slab tangent point. The liner in shear provides the primary load path for the horizontal seismic loads developed in the containment vessel structure. The liner is insulated with a 1-1/4 inch thick layer of polyvinyl chloride (PVC) closed cell foam insulation from the base slab to 15 feet above the spring line. This insulation limits the temperature rise in the liner and the inside surface of the concrete in the cylindrical position of the structure in the event of a LOCA. The liner in the dome, however, is uninsulated. The liner anchorage system in the cylinder consists of 3-inch deep channel sections embedded in the concrete and spaced horizontally approximately 4 feet 4 inches on center. In addition, there are isolated studs in between the channel sections in the cylinder. In the dome, the liner is attached to isolated studs located in a square grid system with 24-inch spacing between studs. There is also a stud in the center of the square.

2.5 DESIGN LOADS

The structure was originally designed using limiting load factors including accident, seismic, and wind loads. The design goal was to assure the structure remained elastic ensuring low strain response. The load combinations used in the design of the containment vessel were:

a. $C = 0.95\ D + 1.5\ P + 1.0\ T$

b. $C = 0.95\ D + 1.25\ P + 1.0\ T' + 1.25\ E$

c. $C = 0.95\ D + 1.0\ P + 1.0\ \underline{T} + 1.0\ E'$

Symbols used in the above equations are defined as follows:

C: Required load capacity of section

D: Dead load of structure

P: Accident pressure load - 60 psig

T: Thermal loads based upon temperature transient associated with 1.5 times accident pressure

T': Thermal loads based upon temperature transient associated with 1.25 accident pressure

$\underline{T}$: Thermal loads based upon temperature transient associated with accident pressure

E: Seismic load based on 0.08g ground acceleration

E': Seismic load based on 0.20g ground acceleration

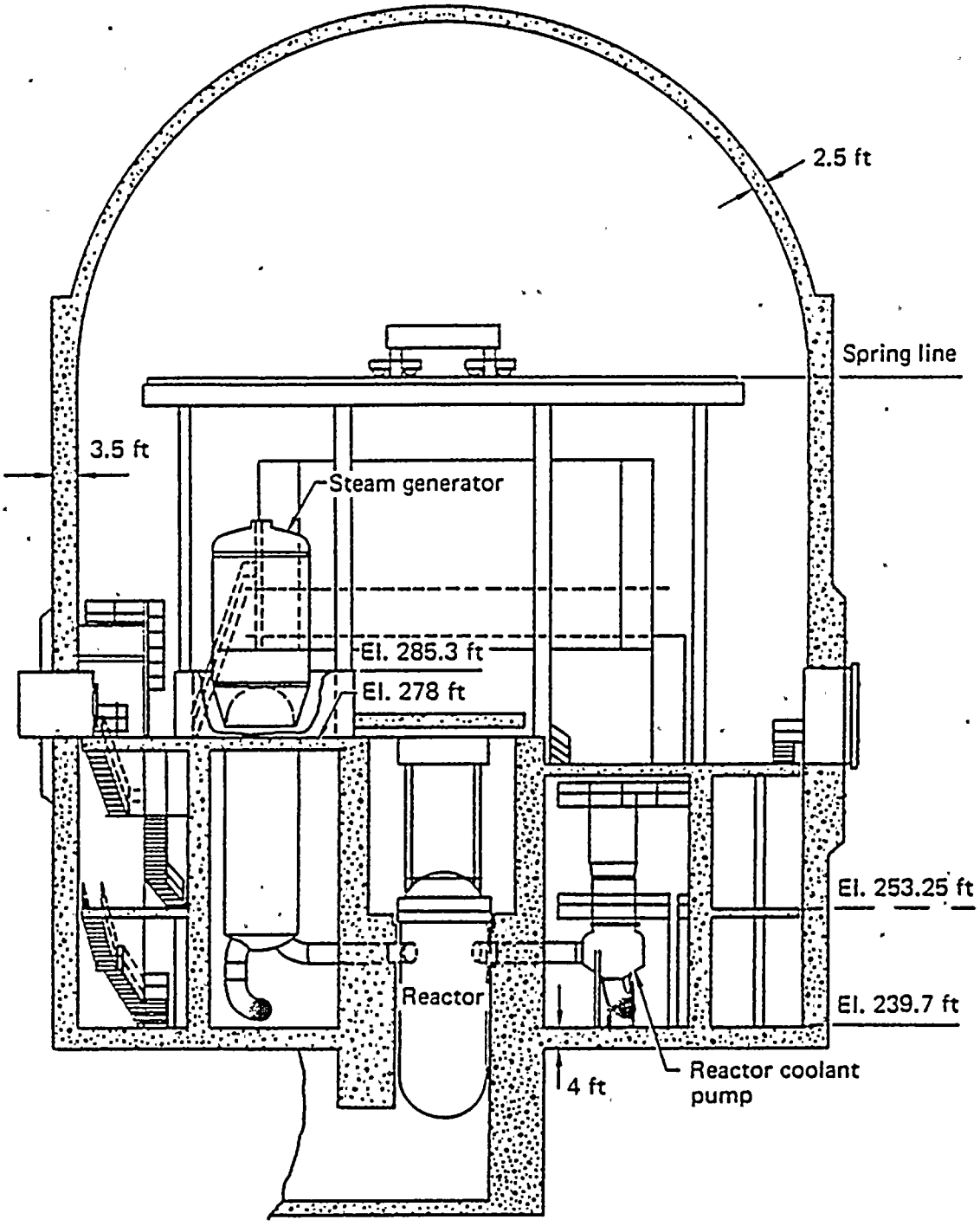

FIGURE 2-1: GINNA REACTOR BUILDING AND EQUIPMENT

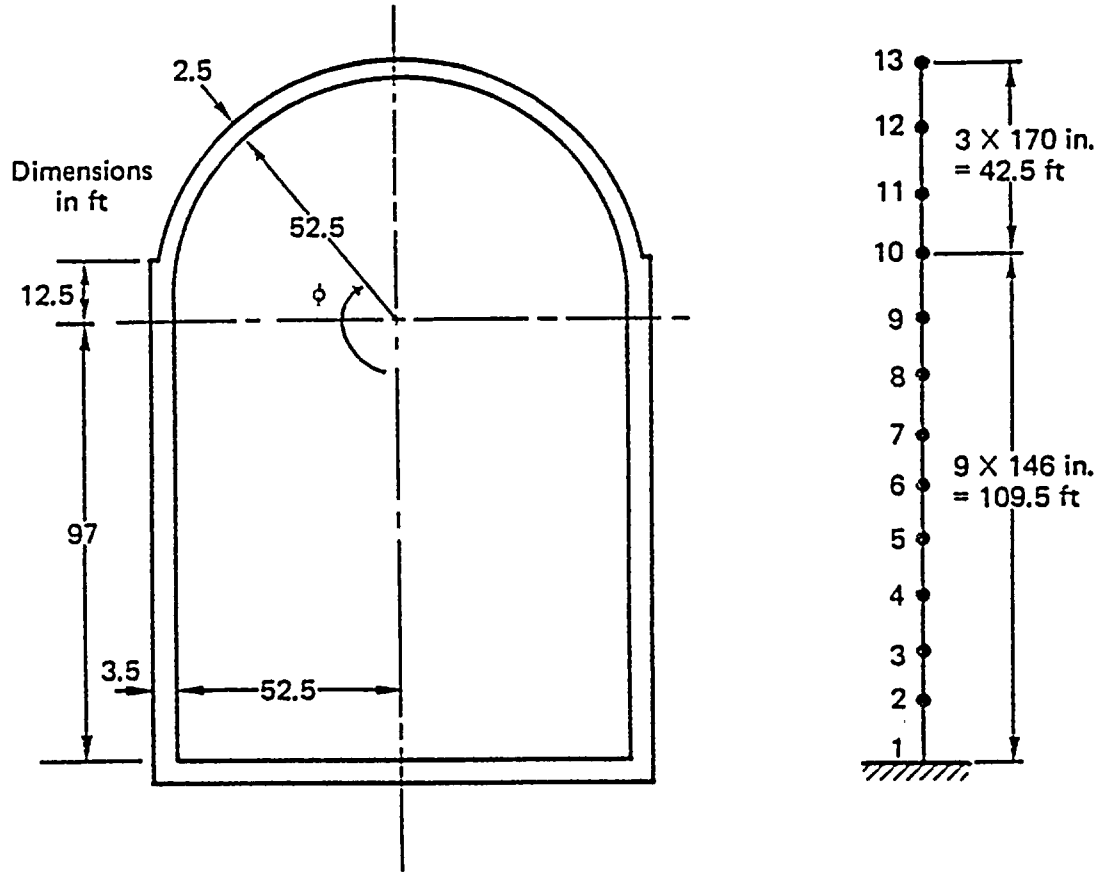

FIGURE 2-2: GINNA REACTOR CONTAINMENT STRUCTURE CONFIGURATION

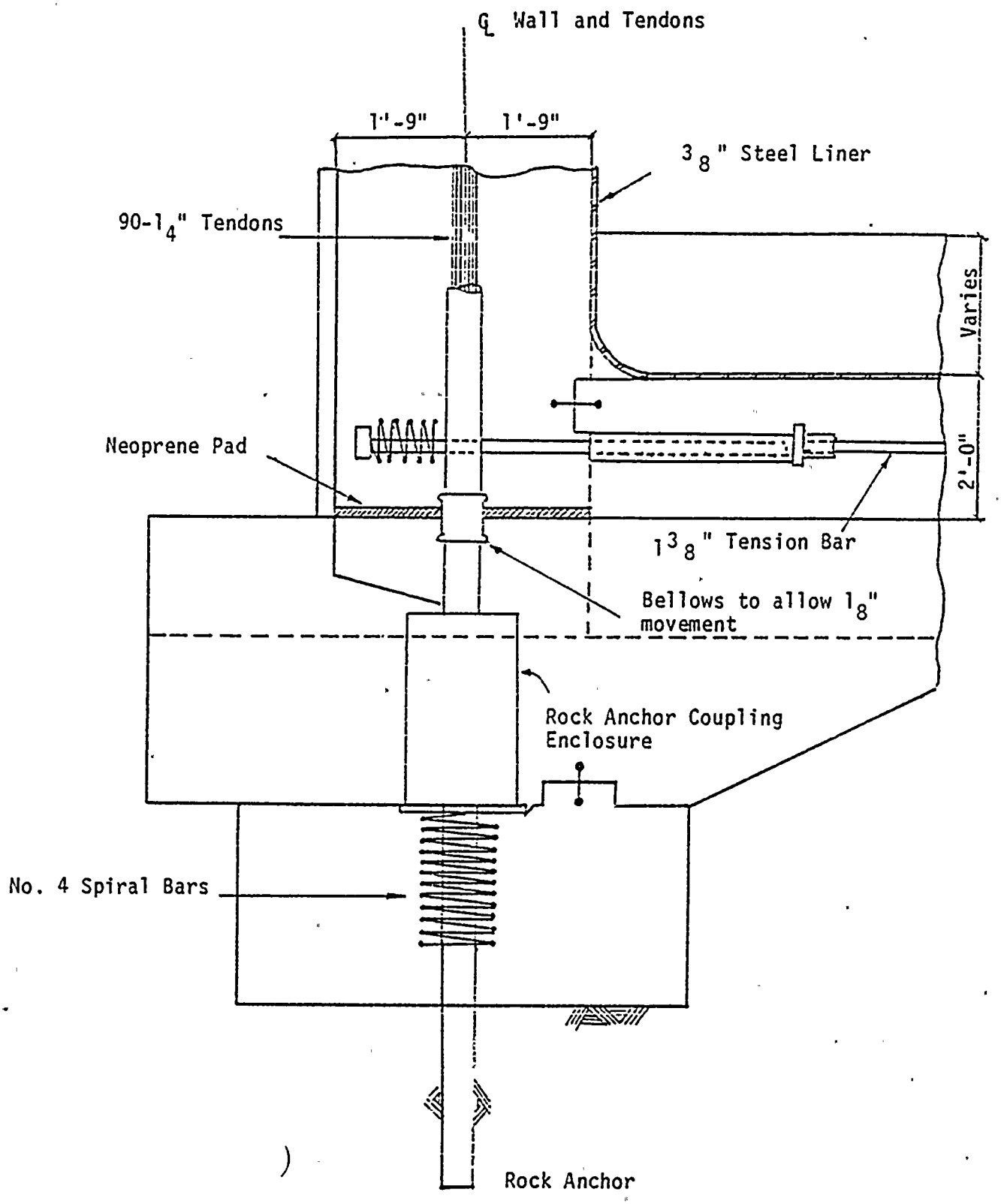

FIGURE 2-3: CONTAINMENT VESSEL - BASE SLAB INTERFACE

3. SEP EVALUATION LOADS

New seismic, thermal, and pressure loads were developed for the Ginna containment structure as part of the SEP program. New seismic loads and the adequacy of the structure to withstand the seismic loads alone were reported in Reference 3. As part of the SEP program, new temperature and pressure time histories were also developed by LLNL (Reference 4). For the SEP evaluation the normal operating loads, peak pressure loads and the thermal loads corresponding to the peak pressure conditions, peak thermal loads and the pressure loads corresponding to peak thermal conditions, and seismic loads were combined. This implies that the SSE occurs approximately 2 minutes after a LOCA. This is considered extremely unlikely and hence the assumed load combination is considered very conservative.

3.1 CONTAINMENT TEMPERATURE

The normal operating temperatures assumed for the Ginna evaluation correspond to a typical "cold day." Ambient temperature inside the reactor building is 110°F and the outside temperature is 2°F. This condition was selected as the operating condition in that thermal gradients and, hence, thermal stresses are expected to be most severe for a cold day. The assumed operating conditions are also the initial conditions for calculating the thermal gradients through the shell. Figure 3-1 shows the transient time history of the containment temperature. A maximum temperature of approximately 421°F is indicated approximately 34 seconds after the start of the transient. However, the internal temperature decreases to less than 300°F at approximately 91 seconds which is the time the peak pressure occurs. The rate of change of temperature compared to the resonant frequencies of the containment is such that the temperature loads may be considered as equivalent static loads.

3.2 CONTAINMENT PRESSURE

Containment pressure corresponding to the accident condition was also developed by LLNL (Reference 4). The time history pressure variation within the containment is shown in Figure 3-2. A maximum pressure of approximately 86 psia occurs at approximately 91 seconds after the start of the transient. Assuming a 14.7 psia ambient pressure results in a pressure difference of 71.5 psig which may be compared with the 60 psig design pressure. The time of maximum pressure does not correspond with the time of maximum temperature. Therefore, a separate load case corresponding to the time of maximum thermal effects on the liner together with the internal pressure at that time was included. Also, the evaluation was conducted for the conditions at 94 seconds rather than 91 seconds. The same peak pressure was used but a computer printout for the liner temperature which controlled the thermal stress results was available at 94 seconds.

3.3 SEISMIC RESPONSE

In the present study, dynamic seismic loads acting on the Ginna containment structure were replaced by a set of equivalent static loads. The equivalent static seismic loads were computed from a previous analysis of the containment structure conducted by LLNL (Reference 3). In the LLNL analysis, the containment shell was modeled as a fixed base system of lumped masses connected by weightless springs (Figure 2-2). Table 3-1 lists the values of masses and characteristics of the connecting beams for the LLNL model. A response spectrum approach was used to determine the dynamic response of the model, i.e., the first ten modal responses of the model were combined using the square-root-of-sum-of-the-squares (SRSS) approach. A USNRC Reg. Guide 1.60 spectrum at 0.2g and 7 percent critical damping was used for the analysis conducted in Reference 3. For the current evaluation, the responses were scaled to a peak ground acceleration of 0.17g in the horizontal direction and 0.11g in the vertical direction. The 0.17g acceleration level is consistent with the site specific SSE for Ginna. Table 3-2 lists modal frequencies of the model, and Table 3-3 shows moment, shear, and axial loads induced in each connecting beam element scaled to 0.17g.

Shear loads in Table 3-3 represent the equivalent static loads for the containment structure. Therefore, the increase in shear between two elevations may be viewed as a uniform lateral load acting on the shell. For the combined pressure, thermal and seismic analysis, the containment shell was modeled as an axisymmetric shell of revolution, and seismic loads acting on the shell were input in accordance with the first harmonic mode shape. Generally, seismic loads on an axisymmetric shell are modeled as a combination of radial and tangential harmonic loads. However, since the circumferential stiffness of the Ginna containment shell is much higher than its radial stiffness, only a tangential load is needed to model the lateral seismic loads. The following relationship may be used to transform a uniform load (F_x) acting between elevations h_1 and h_2 to a harmonic load acting on the shell between the same two elevations:

$$F_x = (h_2-h_1) \int_0^{2\pi} f_x \sin^2 \theta \; r \; d\theta = \pi r \; f_x \; (h_2-h_1)$$

where f_x is the peak harmonic load amplitude and r is the shell radius. For the dome, this relationship may be modified as follows:

$$F_x = \int_0^{2\pi} f_x \sin^2 \theta \; d\theta \int_{\phi_1}^{\phi_2} r \sin \phi \; d\phi$$

$$= \pi r^2 \; f_x \; (\cos \phi_2 - \cos \phi_1)$$

where angle ϕ is defined in Figure 2-2. Harmonic load amplitudes (f_x) for the Ginna containment are listed in Table 3-4.

TABLE 3-1

MASSES, MOMENT OF INERTIA (I), FLEXURAL AREA (A), AND SHEAR AREA (A_s) FOR THE LLNL MODEL

NODE	ELEMENT	MASS $lb\text{-}sec^2/in$	I $in^4(x10^9)$	A $in^2(x10^4)$	A_s $in^2(x10^4)$
13		2480.4			
	12		5.202	12.15	6.074
12		4952.8			
	11		15.35	12.17	6.086
11		4952.8			
	10		21.80	12.08	6.038
10		7007.2			
	9		40.09	19.03	9.516
9		6491.06			
	8		36.44	17.18	8.590
8		5972.0			
	7		36.44	17.18	8.590
7		5972.0			
	6		36.44	17.18	8.590
6		5972.0			
	5		36.44	17.18	8.590
5		5972.0			
	4		36.44	17.18	8.590
4		5972.0			
	3		36.44	17.18	8.590
3		5972.0			
	2		36.44	17.18	8.590
2		5972.0			
	1		36.44	17.18	8.590
1					

TABLE 3-2

MODAL FREQUENCIES FOR THE LLNL MODEL (REF. 3)

MODE	FREQUENCY (CPS)
1	6.97
2	18.87
3	21.47
4	37.75
5	53.91
6	54.60
7	70.23
8	80.89
9	84.70
10	92.38

TABLE 3-3

RESPONSE VALUES FOR THE USNRC REG GUIDE
1.60 HORIZONTAL (0.17g) AND VERTICAL (0.11g) SPECTRA INPUT

ELEMENT	HORIZONTAL		VERTICAL
	MOMENT ($lb\text{-}in \times 10^9$)	SHEAR ($lb \times 10^6$)	AXIAL ($lb \times 10^6$)
12	0.102	0.60	0.204
11	0.391	1.70	0.603
10	0.842	2.68	0.986
9	1.41	3.89	1.50
8	2.12	4.90	1.94
7	2.95	5.71	2.32
6	3.88	6.40	2.65
5	4.90	6.97	2.94
4	5.97	7.42	3.18
3	7.09	7.76	3.37
2	8.24	7.98	3.48
1	9.42	8.08	3.55

TABLE 3-4

PEAK HARMONIC AMPLITUDES OF THE SEISMIC LOAD ON CYLINDER AND DOME OF THE GINNA CONTAINMENT SHELL

*ELEVATION (in.)	LOAD AMPLITUDE (psi)
0	0
73	0.334
219	0.736
365	1.138
511	1.508
657	1.908
803	2.310
949	2.712
1095	5.310
1188	
ϕ (radians)	LOAD AMPLITUDE (psi)
1.57	3.944
1.80	2.074
2.20	2.907
2.62	4.602
3.14	

* Elevation measured from mid-surface of base slab.

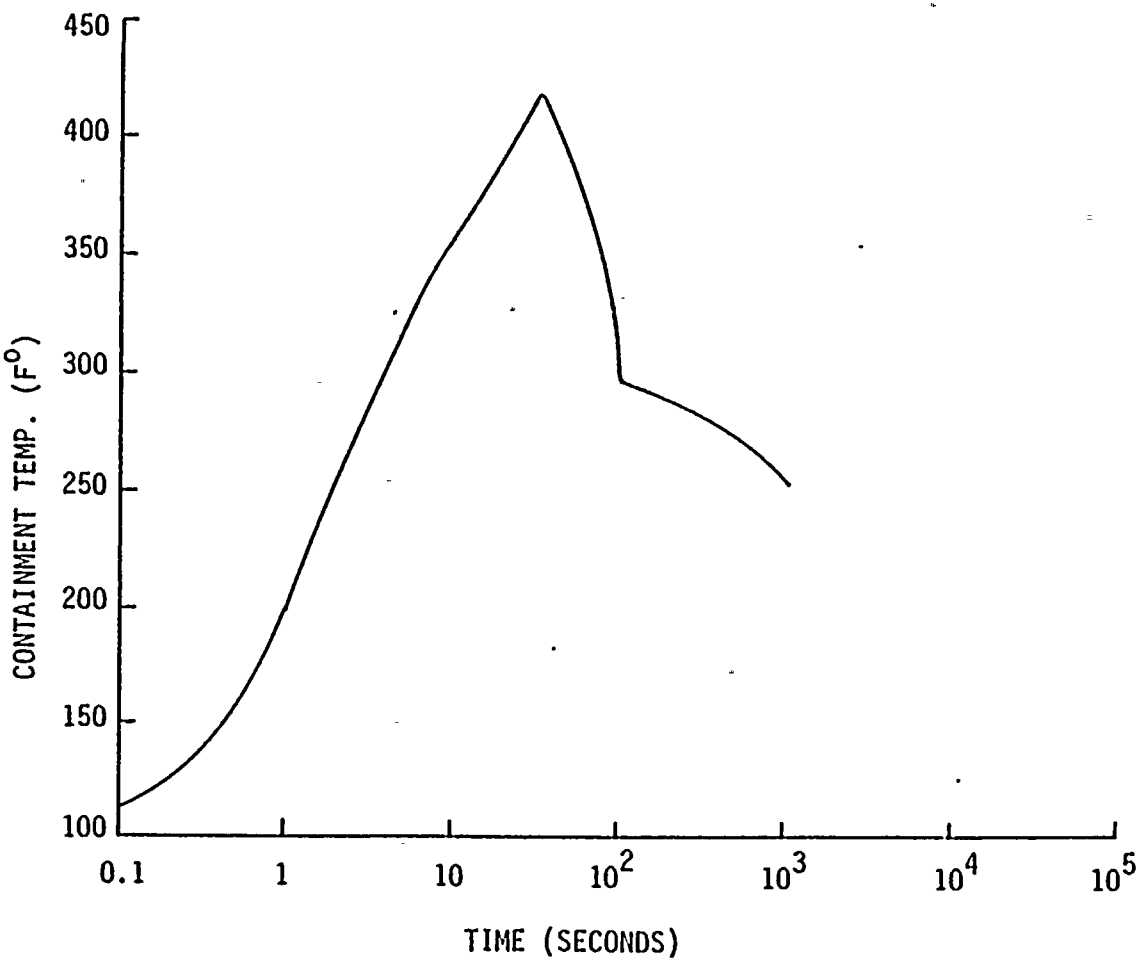

FIGURE 3-1. ACCIDENT TEMPERATURE TRANSIENT INSIDE THE CONTAINMENT

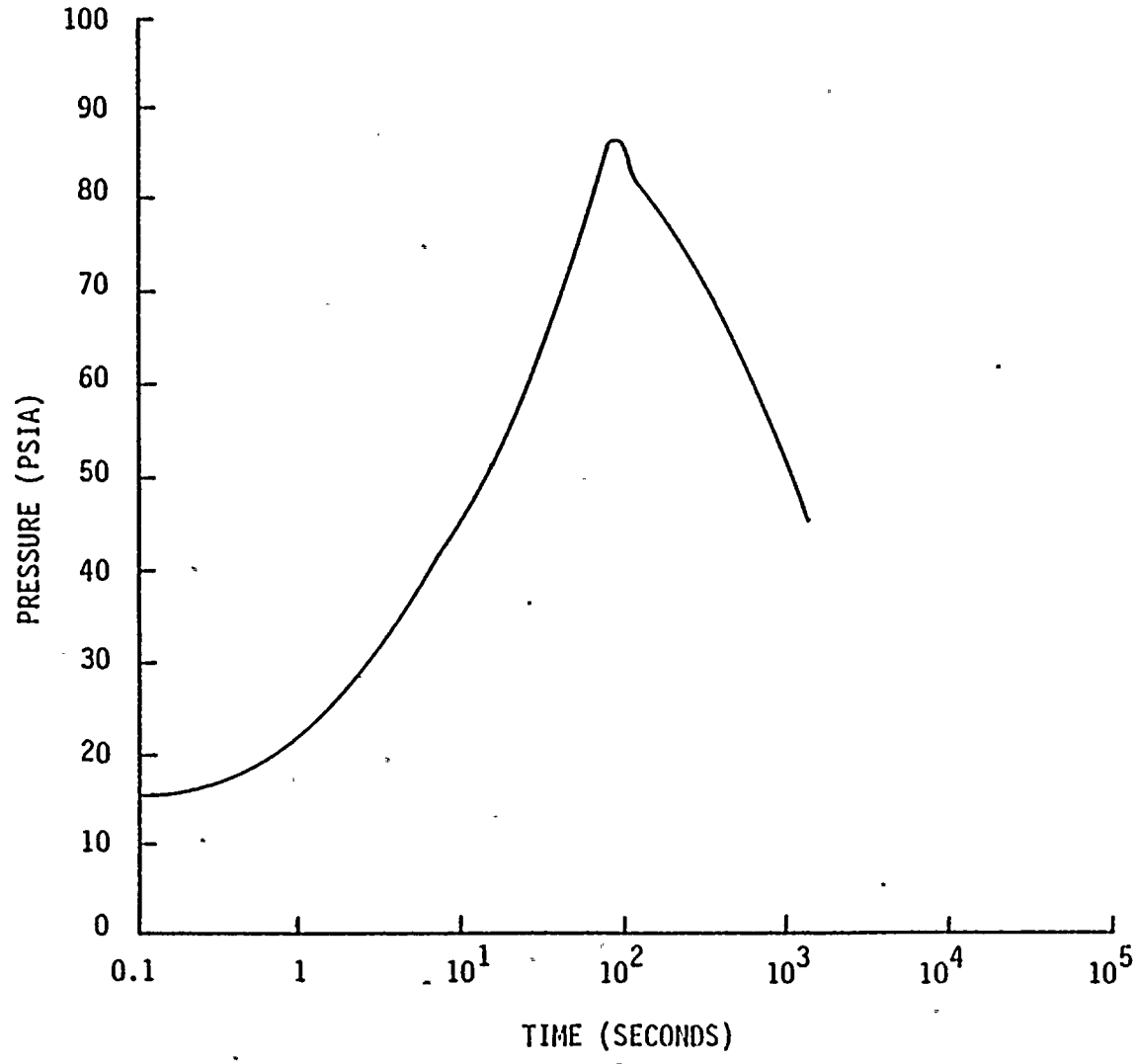

FIGURE 3-2. ACCIDENT PRESSURE TRANSIENT INSIDE THE CONTAINMENT

4. STRUCTURE MODEL DESCRIPTION

The containment structure in the present study was modeled as an axisymmetric shell of revolution. For the current evaluation, no effects of stress concentrations around hatches or penetrations were considered, nor were the details of the hatch and penetration strengths evaluated. The boundary condition at the base of the cylinder was assumed to be simply supported for radial rotation and fixed in the tangential direction. Radial stiffness at the base was computed to be 46.9 kip/in./in. This is the stiffness of the radial tension bars anchoring the shell to the base slab, which are partially free to deform under tangential loads.

Two different computer codes were used to carry out the analysis. The computer program ANSYS (Reference 5) was used to determine the temperature gradient through the shell for steady-state (normal operating) temperature and the transient temperature conditions. Once the temperatures in the shell were determined, the computer program FASOR, Field Analysis of Shells of Revolution (References 6 and 7) was used to calculate displacements, stresses, and stress resultants under various loading conditions. FASOR employs a numerical integration method called the "field method" to solve the differential equations of a shell. A shell in FASOR may be modeled as a multilayer shell of revolution, where the thickness material properties and temperatures for each layer are specified separately. The shape of a shell may be described as a general arc so that there is no need to discretize the shell into small elements. The program defines integration points along the shell from an error tolerance specified by the user.

For pressure, seismic loads, and operating temperature loads, the shell was modeled as two-layers, i.e., a 0.375-inch-thick layer of steel connected to a layer of concrete. The concrete thickness changes from 42 inches in the cylinder to 30 inches in the dome. Concrete

and steel material properties are listed in Table 4-1. For accident temperature loads, the shell was modeled as three layers, i.e., the steel liner and two layers of concrete. The temperature gradient through each layer was assumed to be linear. The boundary condition at the base was assumed to be fixed in the tangential direction. Radial stiffness at the base was computed to be 46.9 kip/in./in. as discussed above.

Preliminary analysis indicated that the insulation is effective in limiting the heat flow through the cylindrical portion of the structure and maintaining the insulated liner at a significantly lower temperature than occurs in the uninsulated liner in the dome. For example, for normal operating temperature loads of 110°F ambient air temperature inside and 20°F air temperature outside, the liner temperature in the uninsulated part of the dome is approximately 102°F On the other hand, in the insulated cylinder the liner temperature is limited to approximately 69°F. This was verified by an LLNL analysis where temperature of the inside surface of liner and effective film coefficients were computed throughout the containment for the transient thermal loads. This temperature includes the temperature drop through the film coefficient at the liner inside surface. In order to develop the thermal gradients through the shell, a transient thermal analysis was performed using ANSYS (Reference 5) with the inside liner surface temperature developed by LLNL specified as a boundary condition. As expected, it was found that the insulated part of the containment shell remains close to its steady-state condition throughout the transient time period. On the other hand, temperatures of the uninsulated liner as well as a very thin layer of the concrete containment next to the liner increase significantly as a result of internal transient air temperature. Figures 4-1 and 4-2 show the temperature gradient through the liner and adjacent concrete 94 seconds and 380 seconds after the start of the accident. Figure 4-1 corresponds to the time of peak pressure and Figure 4-2 corresponds to the peak liner temperature during the accident. As may be seen in Figures 4-1 and 4-2, only a thin layer of concrete is effected by the temperature rise, i.e., approximately 0.25 inches at 94 seconds and 0.8 inches at 380 seconds.

Although this part of the concrete has only a small effect on the overall shell response; it was included as a separate layer in the analysis. The containment shell was therefore modeled as a three-layer shell consisting of the steel liner and two layers of concrete. The temperature gradient was assumed linear in each of the layers. For the insulated liner, the liner temperature stays approximately at 69°F throughout the accident. The outer concrete surface temperature for both insulated and uninsulated parts of the containment was calculated to be approximately 10°F.

TABLE 4-1

MATERIAL PROPERTIES FOR STEEL, CONCRETE, AND FOAM INSULATION

	Steel Liner	Concrete	Insulation	Reinforcement Steel
Young's Modulus (psi)	29×10^6	4.3×10^6	-	29×10^6
Poisson's Ratio	0.3	0.25	-	-
Coefficient of Thermal Expansion (in/in)F°	6.3×10^{-6}	5.5×10^{-6}	-	-
Density (lbs/cu. ft)	490	150	4	-
Coefficient of Thermal Conductivity BTU/hr. ft, F°	26	0.44	0.022	-
Specific Heat BTU/lb_mF°	0.11	0.160	0.30	-
Thickness (in)	0.375	42-30	1.25	-
σ_Y (psi) Steel f'_c (psi) Concrete	32,000	5,000	-	40,000

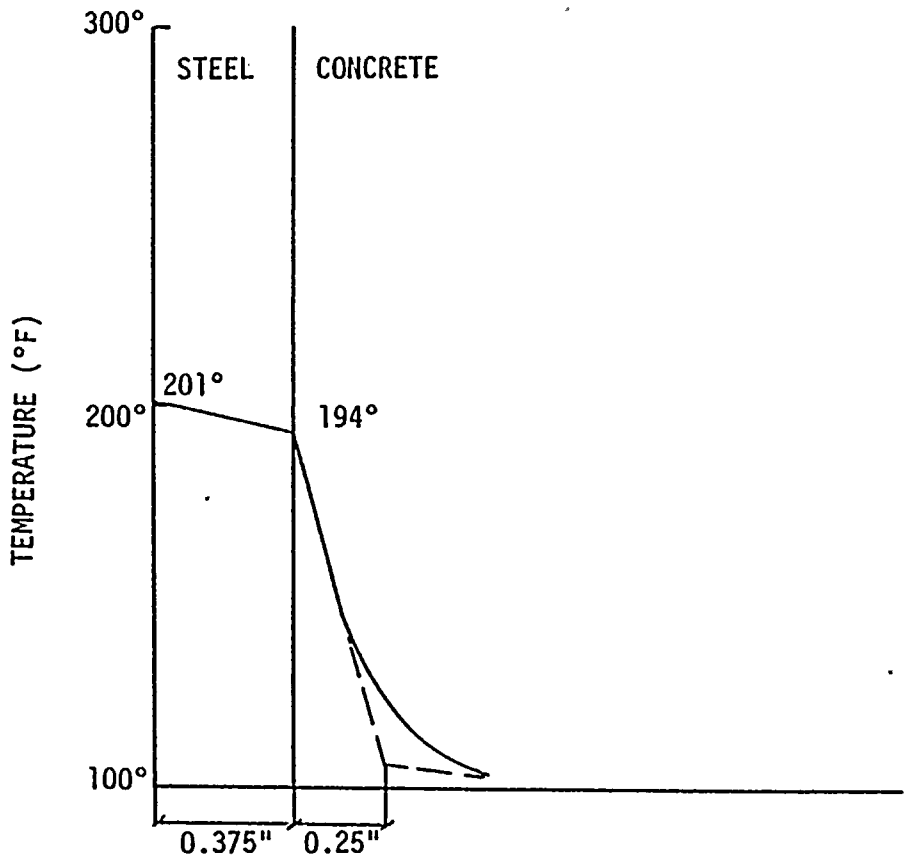

FIGURE 4-1: ACCIDENT TEMPERATURE GRADIENT THROUGH THE UNINSULATED CONTAINMENT SHELL AFTER 94 SECONDS

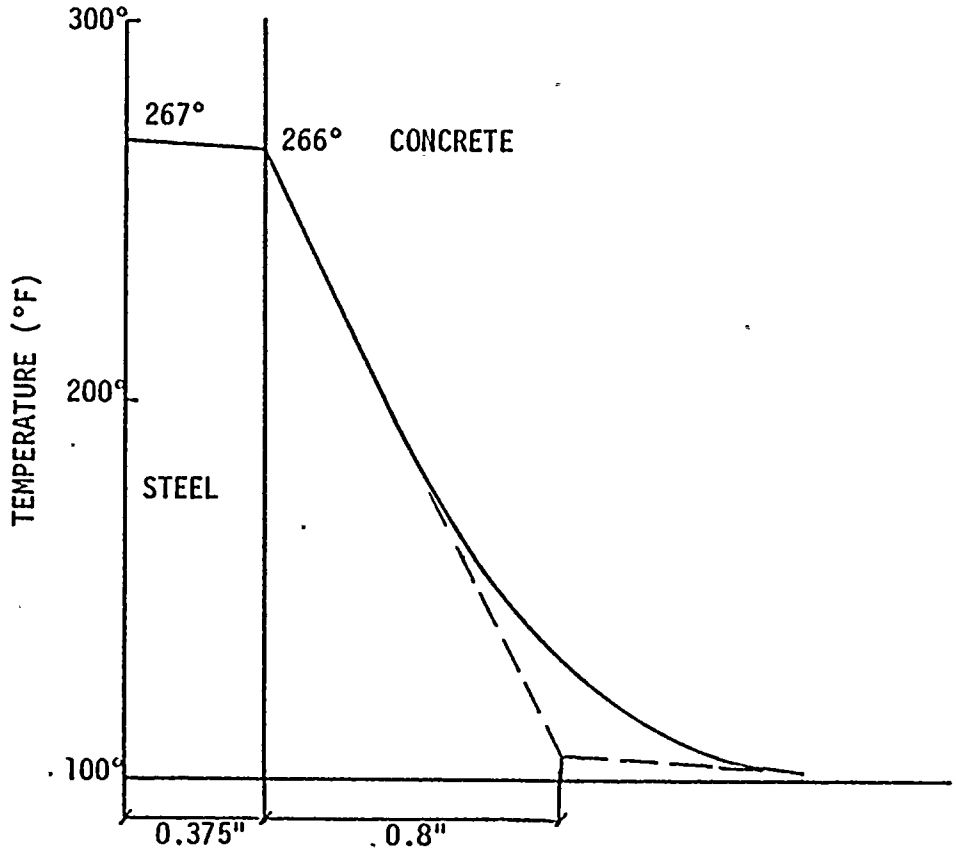

FIGURE 4-2: ACCIDENT TEMPERATURE GRADIENT THROUGH THE UNINSULATED CONTAINMENT SHELL AFTER 380 SECONDS

5. SHELL RESPONSE

This section presents response of the containment shell subjected to operating loads, accident loads, and their combinations. Operating loads consist of the dead weight, prestress load, and normal temperature. Earthquake loads, accident temperature, and accident pressure were the accident loads considered in the present study. The following load combinations were considered:

a. $C = D + P + E$

b. $C = D + P + E + T_a$

where

C = Required load capacity of section

D = Dead load and prestress load

E = SSE-based seismic load (0.17g)

P = Accident pressure load

T_a = Accident temperature load

Although Case a. is physically impossible since the accident pressure cannot occur without the corresponding accident temperature, it was included to provide a comparison with the design load combination results. This was done because of the uncertainty of how the accident temperature loads were accounted for in the design analysis. Case b. was considered at two different times during the transient, i.e., at 94 seconds and at 380 seconds. The former corresponds to the time of peak pressure and the latter corresponds to the time of peak temperature in the liner. Except for the deadweight and prestress load (D), response of the axisymmetric containment shell to other loads was computed using the computer program FASOR.

Figure 5-1 shows the containment displacement, radial shear, meridional moment, and tangential shear under seismic loads. Since the seismic load acts primarily as a tangential harmonic load on the shell, very little meridional moment and radial shear were induced. The sign convention used is that a positive radial shear indicates a shear load which points towards the center of the shell.

Figures 5-2 through 5-4 show the containment response for operating and accident temperatures. It is clear from these figures that the effect of accident temperature is mainly in the uninsulated part of the dome. For example, the meridional moment increases from 290 kip-ft/ft for the operating temperature to a peak value of 551 kip-ft/ft after 380 seconds. On the other hand, the moment in the cylinder remains at approximately 400 kip-ft/ft throughout the transient.

Response parameters along the containment for accident pressure loads of 86 psia and 69 psia apear in Figures 5-5 and 5-6. Since the results are based on elastic analysis, the shapes of response parameters along the containment shell in these two figures are identical. Containment axial response to deadweight and prestress loads were computed to be 74 kip/ft and 299 kip/ft, respectively (Figure 5-7). Since it is unlikely that peak horizontal and peak vertical seismic loads happen at the same time, they were combined using the SRSS method. Figure 5-7 indicates that with the pressure load and seismic loads acting upwards, there is very little additional margin of safety available to resist containment uplift in the case of a combined seismic event and LOCA. However, even if the prestress and deadweight loads should be overcome over a small segment of the shell, the vertical tendons will remain intact, and the liner knuckle flexibility will provide for some uplift before liner failure is expected. The seismic response of the structure for this case was based on the assumed 7 percent damping as discussed in Reference 3. To determine the required limiting capacity of the shell, two load combinations were considered. Figure 5-8 shows the containment response to D + P + E loads. Radial shear, moment, and hoop tension are

dominated by the peak pressure load (86 psia), while tangential shear is mainly due to the seismic lateral loads. Figure 5-9 shows the results for the $D + P + E + T_a$ load combination at the time of peak pressure, and Figure 5-10 is the response to the same load combination at the time of peak liner temperature. A comparison of Figures 5-8, 5-9, and 5-10 reveals that displacement and meridional moment in the shell are very much effected by the transient accident temperature. For purposes of comparison, the original design load combination is depicted in Figure 5-11. The peak response parameters, especially hoop tension and meridional moment in the dome, are higher than their original design values. It should be noted that the high meridional moment in the dome is mainly due to the thermal gradient through the shell which has a self-limiting effect due to shell cracking. However, it is not clear how the moment due to the thermal gradient was considered in the original design analysis.

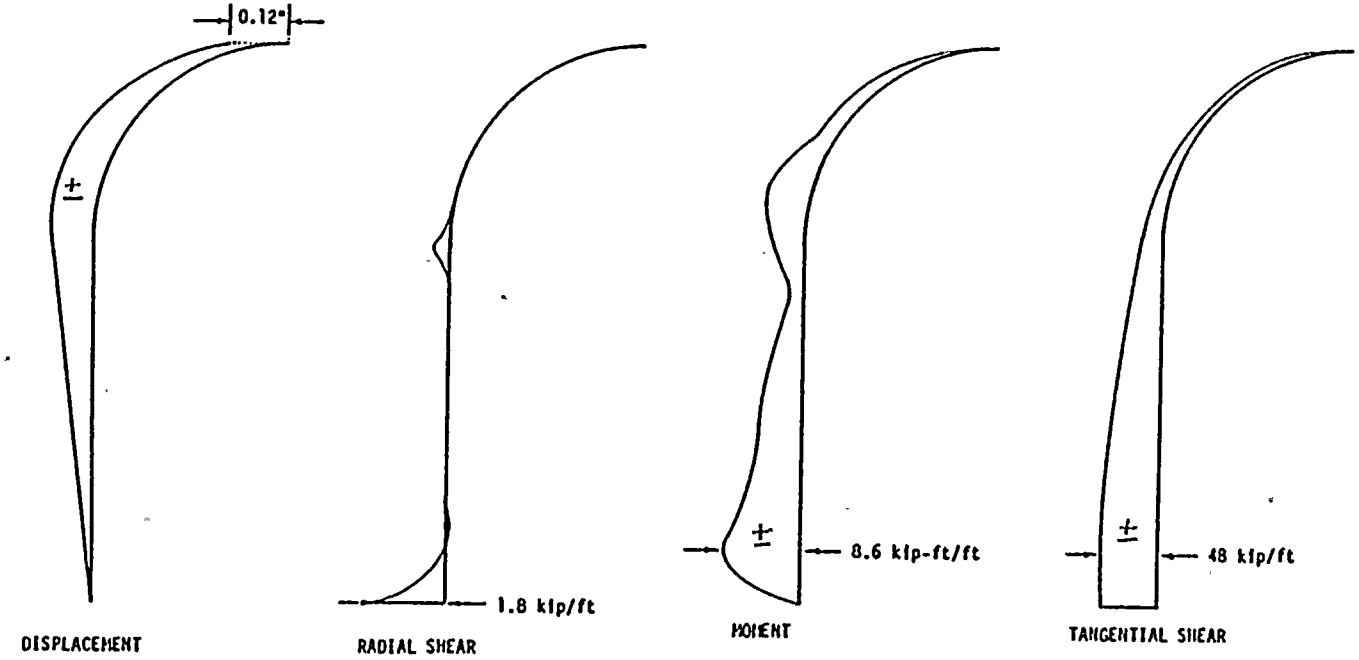

FIGURE 5-1. CONTAINMENT RESPONSE FOR SSE (E)

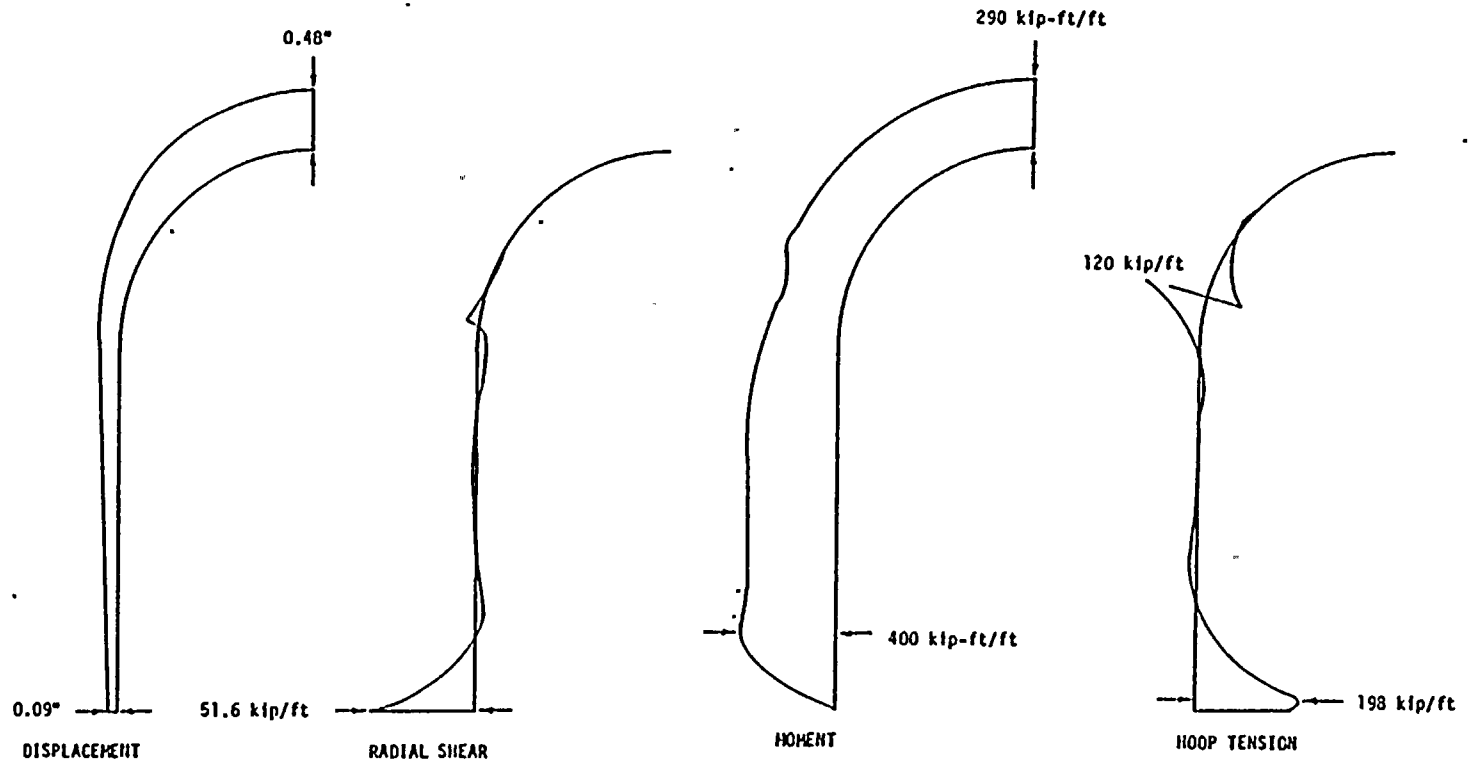

FIGURE 5-2. CONTAINMENT RESPONSE FOR OPERATING TEMPERATURE (T_o)

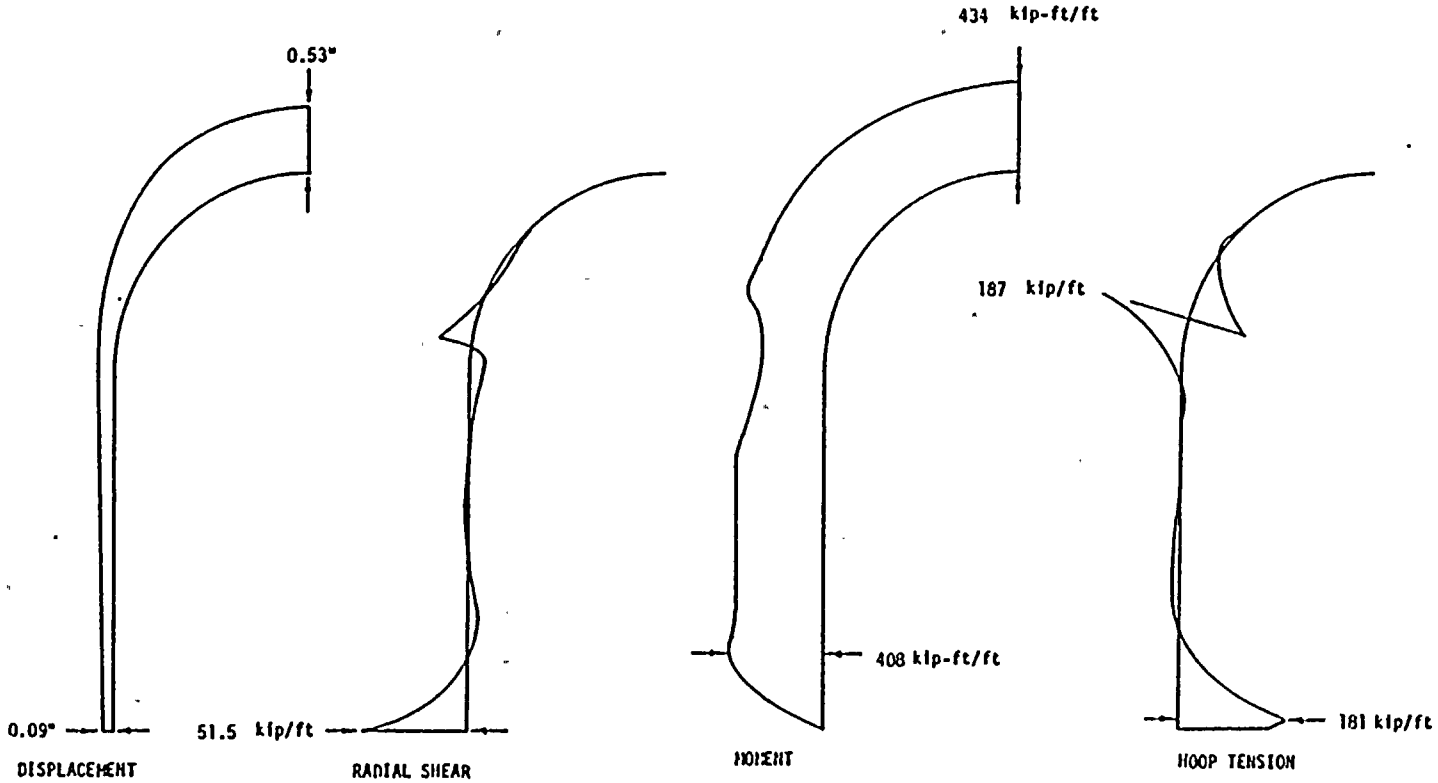

FIGURE 5-3. CONTAINMENT RESPONSE FOR ACCIDENT TEMPERATURE (T_a) AT T = 94 SECONDS

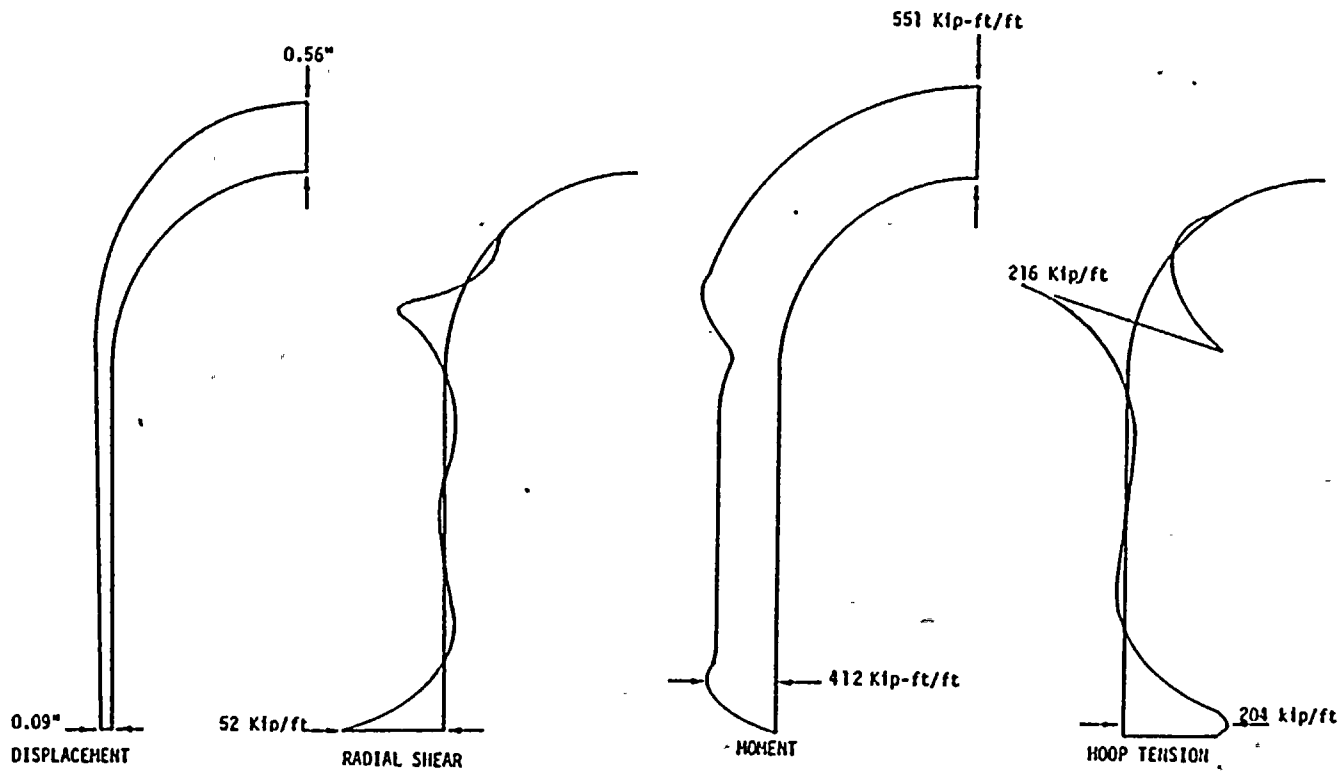

FIGURE 5-4. CONTAINMENT RESPONSE FOR ACCIDENT TEMPERATURE (T_a) AT T = 380 SECONDS

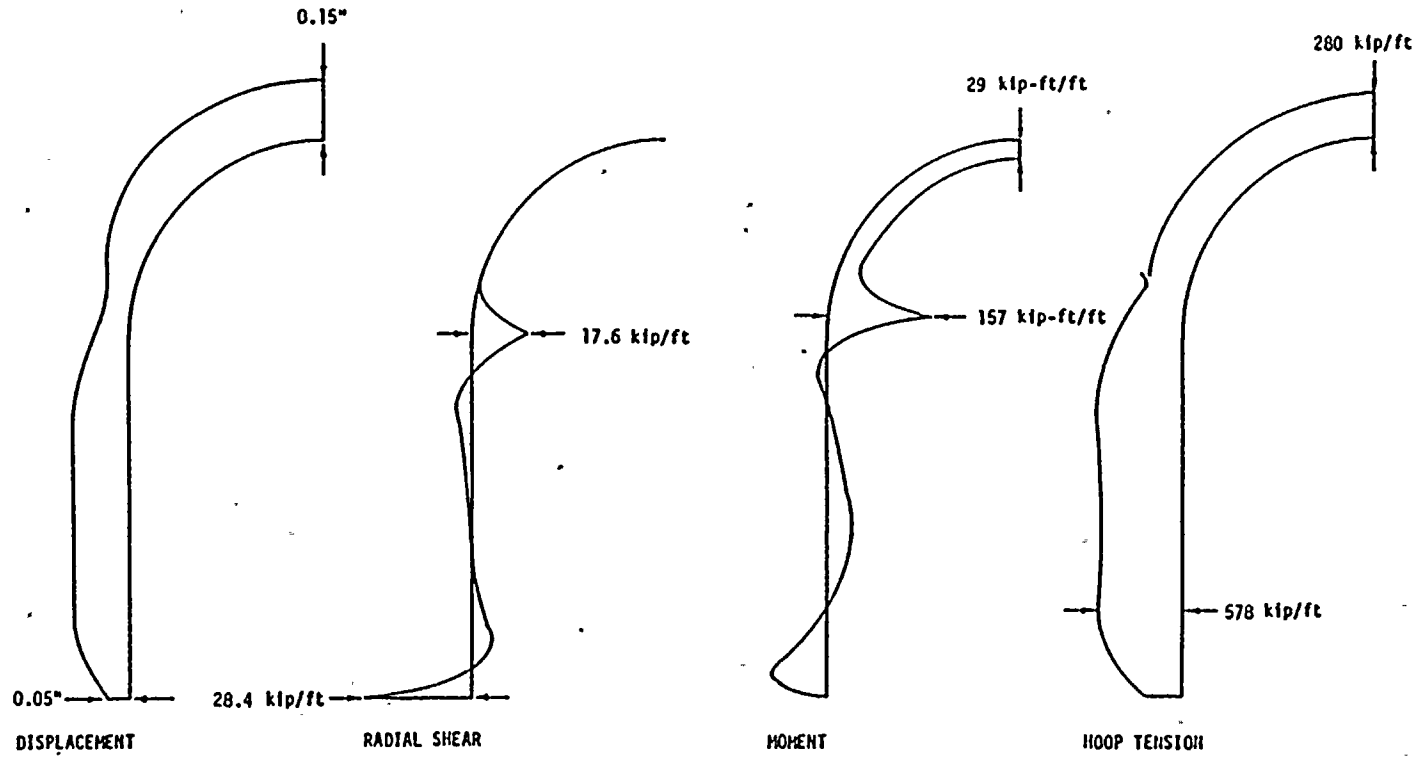

FIGURE 5-5. CONTAINMENT RESPONSE FOR ACCIDENT PRESSURE (P = 86 PSIA) AT T = 94 SECONDS

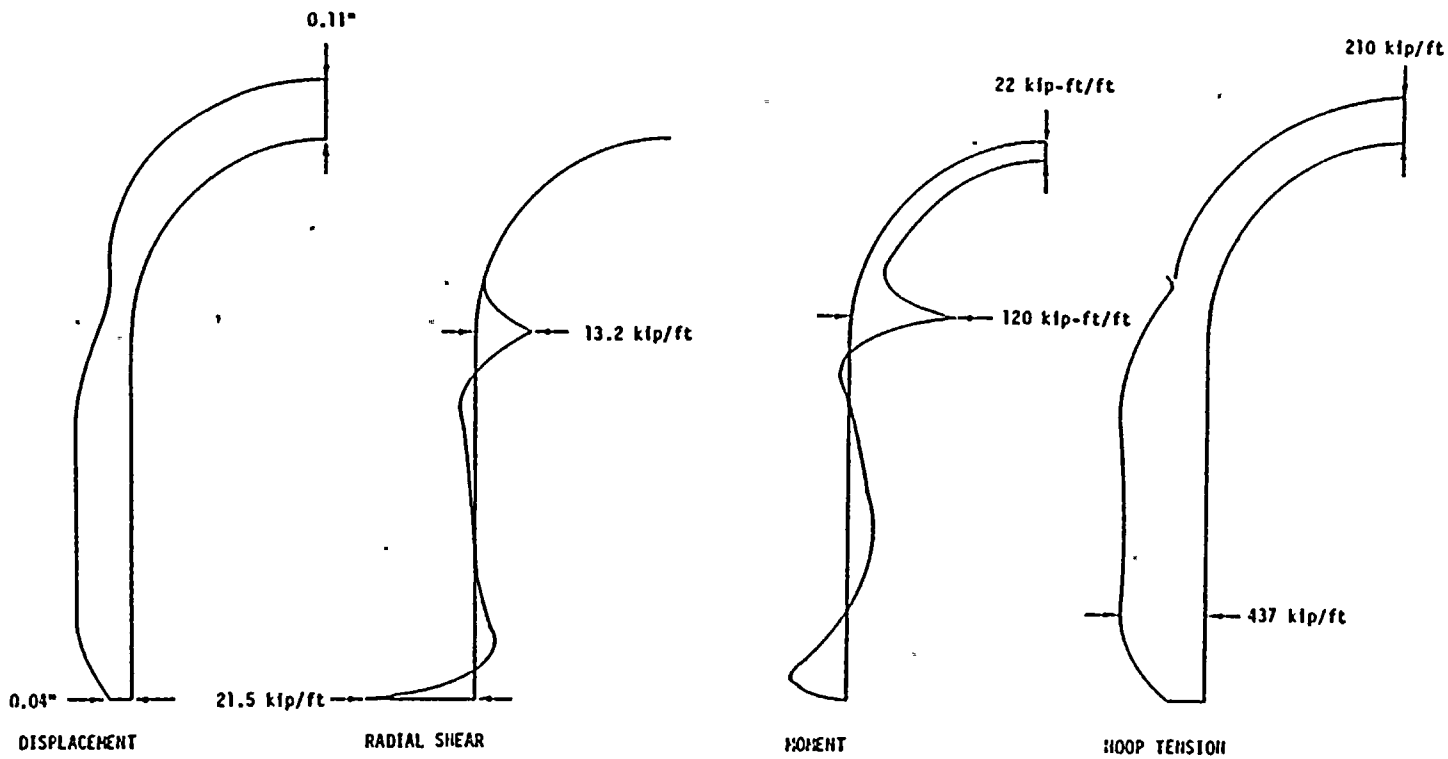

FIGURE 5-6. CONTAINMENT RESPONSE FOR ACCIDENT PRESSURE (P = 69 PSIA) AT T = 380 SECONDS

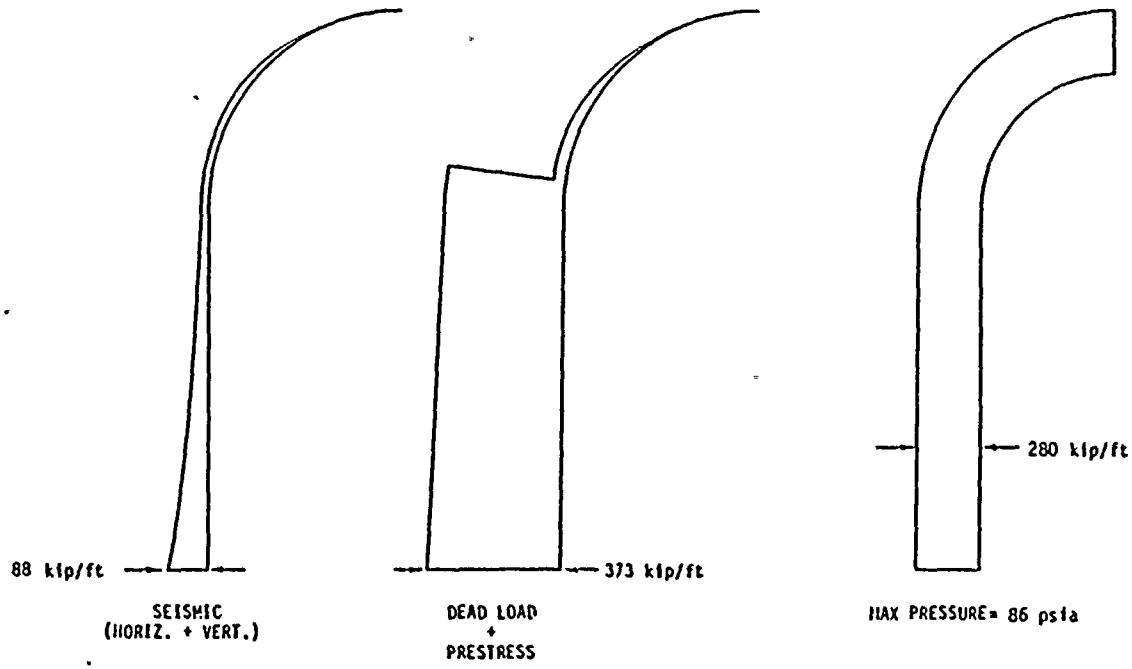

FIGURE 5-7. CONTAINMENT AXIAL RESPONSE (E, D, P)

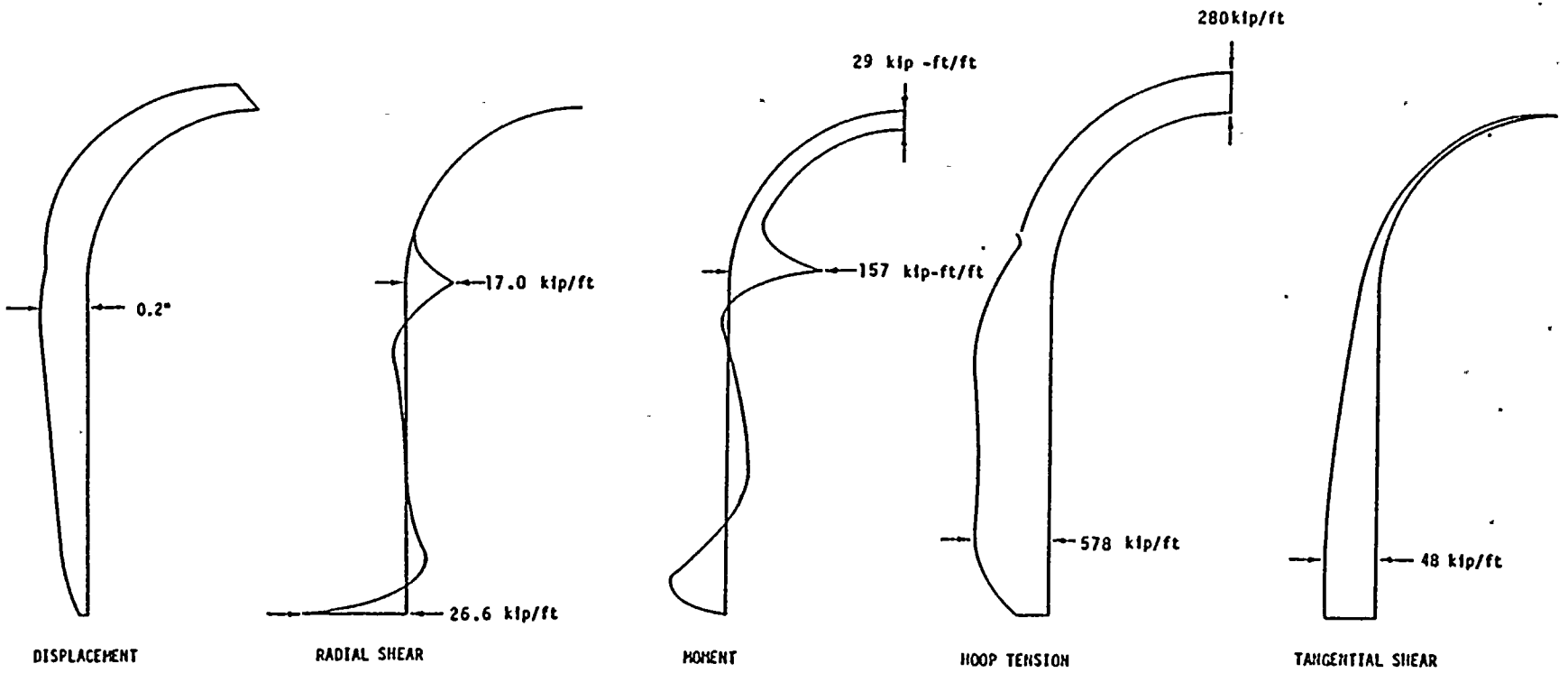

FIGURE 5-8: CONTAINMENT RESPONSE FOR DEAD LOAD (INCLUDING PRESTRESS) PLUS PRESSURE PLUS SSE (D + P + E)

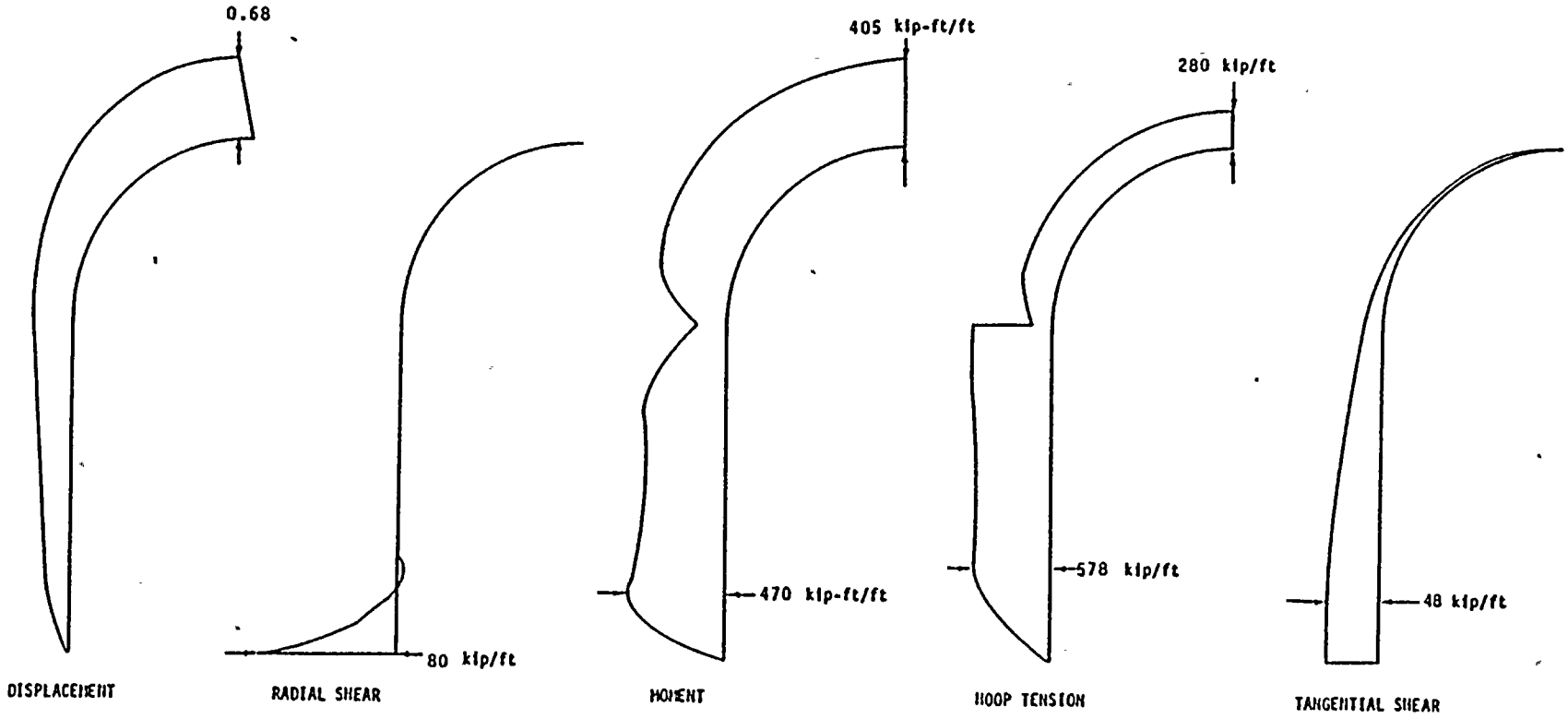

FIGURE 5-9. CONTAINMENT RESPONSE FOR DEAD LOAD (INCLUDING PRESTRESS) PLUS PRESSURE PLUS SSE PLUS ACCIDENT TEMPERATURE ($D + P + E + T_a$) AT T = 94 SECONDS

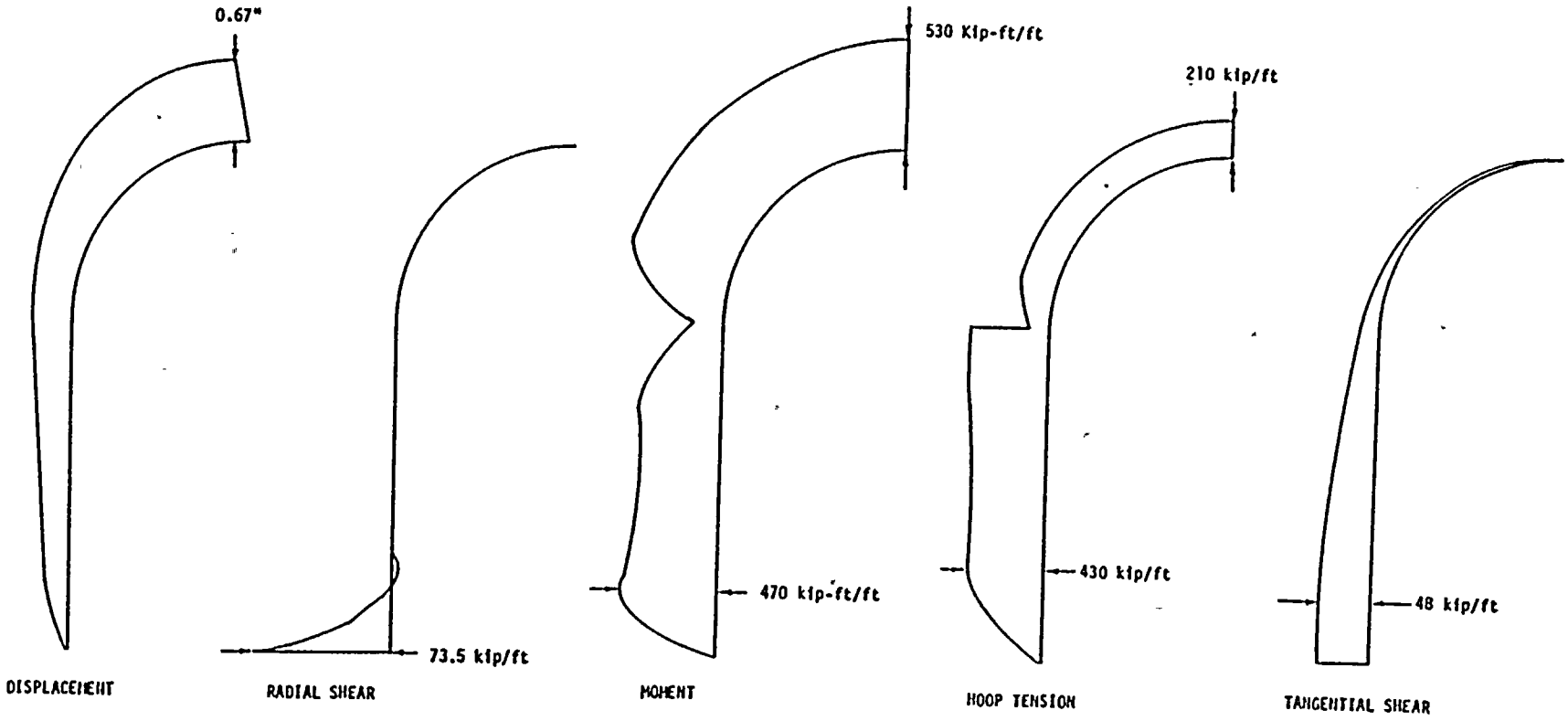

FIGURE 5-10. CONTAINMENT RESPONSE FOR DEAD LOAD (INCLUDING PRESTRESS) PLUS PRESSURE PLUS SSE PLUS ACCIDENT TEMPERATURE ($D + P + E + T_a$) AT T = 380 SECONDS

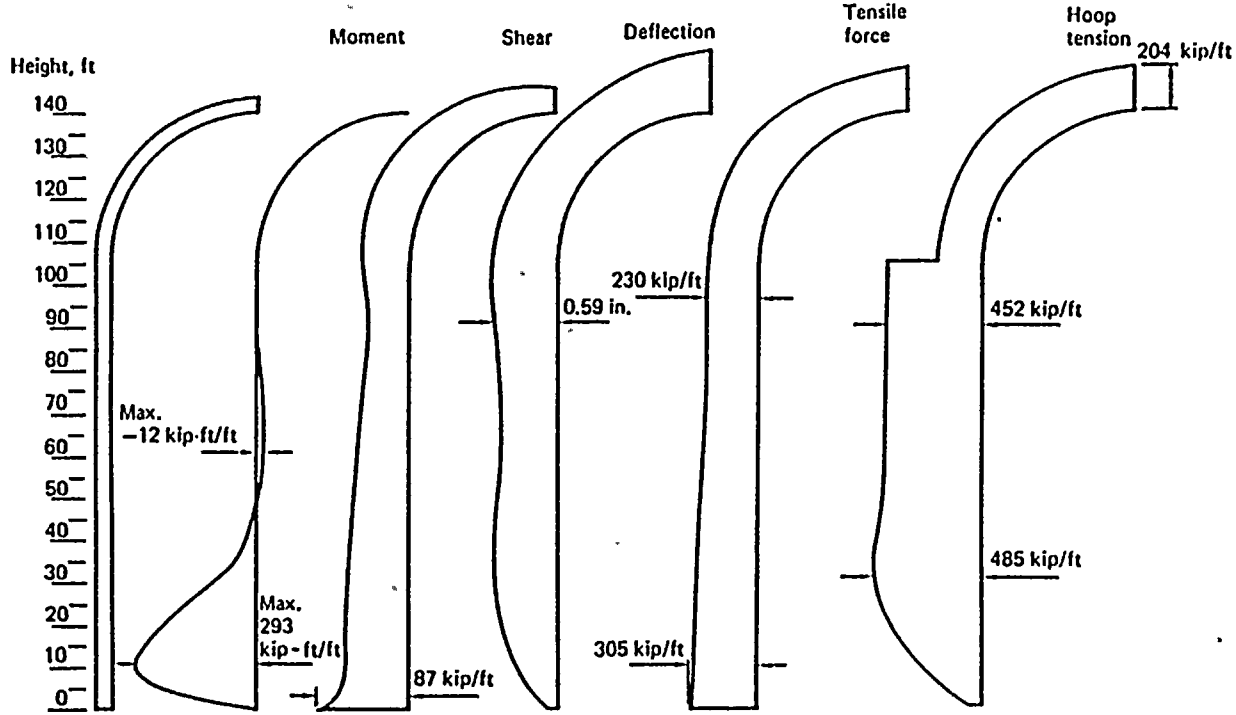

FIGURE 5-11. ORIGINAL DESIGN LOAD COMBINATION FOR 95 PERCENT DEAD LOAD PLUS PRESSURE PLUS SEISMIC PLUS ACCIDENT TEMPERATURE ($0.95D + P + E + T_a$)

6. STRESSES

Responses of the containment shell under various loads and their combinations were presented in the previous chapter. The results were based on an elastic uncracked-section analysis of the axisymmetric containment shell. In the present chapter, both elastic shell stresses and steel and concrete stresses computed from a cracked section analysis of the dome are presented.

6.1 SHELL STRESSES

The shell stresses presented in this section were calculated from response moments, shears, and axial loads shown in Chapter 5 assuming that the strains vary linearly across each layer, i.e., no concrete cracking is considered. The results throughout the cylinder and dome, except for deadweight and prestress load, are presented graphically in Figures 6-1 through 6-17. The combination of deadweight and prestress loads are most significant near the base and induce a maximum compressive stress of 0.7 ksi in the concrete and 5.3 ksi in the steel liner. In Figures 6-1 through 6-17, the cylinder height is 1188 inches and the insulation extends approximately 180 inches above the spring line. It is clear from these figures that the steel and concrete stresses are most critical in the uninsulated part of the dome where the transient thermal loads become important. In comparison, maximum seismic stresses in the liner and concrete are very small in relation to the pressure and temperature stresses.

6.2 CRACKED SECTION ANALYSIS

In order to check the stresses in concrete and reinforcing steel in the dome, a cracked section analysis based on simple elastic bending theory was carried out. The analysis is for the peak temperature loads which correspond to a pressure load of 69 psia at 380 seconds after the start of the accident. The following approach was used to calculate the stresses.

1. Axial Load

It is clear from Figures 5-1 through 5-10 that the only important axial load in the dome is due to the pressure, P_c, which is reacted at the center of the cracked section.

2. Moment

a. The moment due to the pressure axial load, M_c, varies with the location of the center of cracked section

$$M_c = P_c\ (t/2-d_o)$$

where t is the thickness of the section and d_o is the distance to the center of gravity of the cracked section (Figure 6-18).

b. Moment due to thermal loads, M_t, is proportional to the cracked moment of inertia.

$$M_t = (I_c/I_o)\ M_{to}$$

where I_o is the initial (uncracked) moment of inertia. Other moments in the dome are quite small and therefore, disregarded.

Also, from the section properties, the following relationships hold.

$$I_o = bt^3/12$$

$$A_c = bkd + nA_s + (n-1)\ A_s'$$

$$n = E_s/E_c$$

$$d_o = [\tfrac{1}{2} b (kd)^2 + (n-1) A_s' d' + n A_s d]/A_c$$

$$I_c = \tfrac{1}{12} b (kd)^3 + bkd (d_o - \tfrac{kd}{2})^2 + (n-1)A_s' (d_o - d')^2 + nA_s (d - d_o)^2$$

where b is the width, kd is the distance from compression fiber to the neutral axis, A_s is the tensile steel area, A_s' is the compressive steel area, E_s is the steel modulus of elasticity, and E_c is the concrete modulus of elasticity. From section equilibrium:

$$M_c + M_t = F_c (t/2 - kd/3) + F_s (d - t/2)$$

$$P_c = F_c + F_s$$

where F_c and F_s are concrete and steel forces, respectively. The above equations were solved by trial and error, i.e., assuming a value of k and computing a new value from equilibrium equations. The results show that the maximum stress in the main reinforcing steel in the dome is 12.8 ksi which is much lower than the ASME code allowable of 0.9 σ_y = 36 ksi. Also, the peak stress in the welded wire fabric which is placed towards the outer surface of the containment shell is below the steel yield stress. Maximum concrete compressive stresses were computed to be 3700 psi which is less than the code allowable of 0.85 f_c' = 4250 psi.

6.3 LINER STRESSES

The horizontal seismic shear loads (Figure 5-1) are primarily resisted by the liner in shear through the knuckle into the base slab. Other load paths include the shear transfer through the neoprene pads and the radial shear through the radial rods which anchor the base slab to the vessel wall. The stiffnesses computed for neoprene pads and the rods are much smaller than the stiffness of the liner knuckle in shear, however, and it was conservatively assumed in this evaluation that all the horizontal shear force from the containment vessel is transferred to

the base slab through the liner. The load distribution is expected to be the first harmonic as in the wall. The maximum shear stress in the liner was computed to be approximately 21,000 psi. The minimum tensile yield strength of the liner material is 32,000 psi. Using the AISC code allowable shear strength of 0.60 σ_y, or approximately 19,200 psi, some very localized yielding of the liner is indicated based on these minimum material properties.

6.4 TENSION ROD STRESSES

The radial loads (Figure 5-9), on the other hand, are resisted by the radial tension rods in the outward direction, while the radial loads in the inward direction are resisted by the concrete base slab in bearing. The thermal and pressure LOCA loads result in radial expansion and, hence, tension in the rods. The stiffness of the liner knuckle in the radial direction is very low compared to the rods and virtually no radial loads are transmitted through the liner. The maximum tensile stress computed in the rod for the combined load case in Figure 5-9 is approximately 54,000 psi. No shear stress is developed in the rods due to the clearance between the rod and sleeve in the base slab. The minimum tensile yield strength in the rods is 130,000 psi so that a factor of safety of approximately 2.6 exists for this detail.

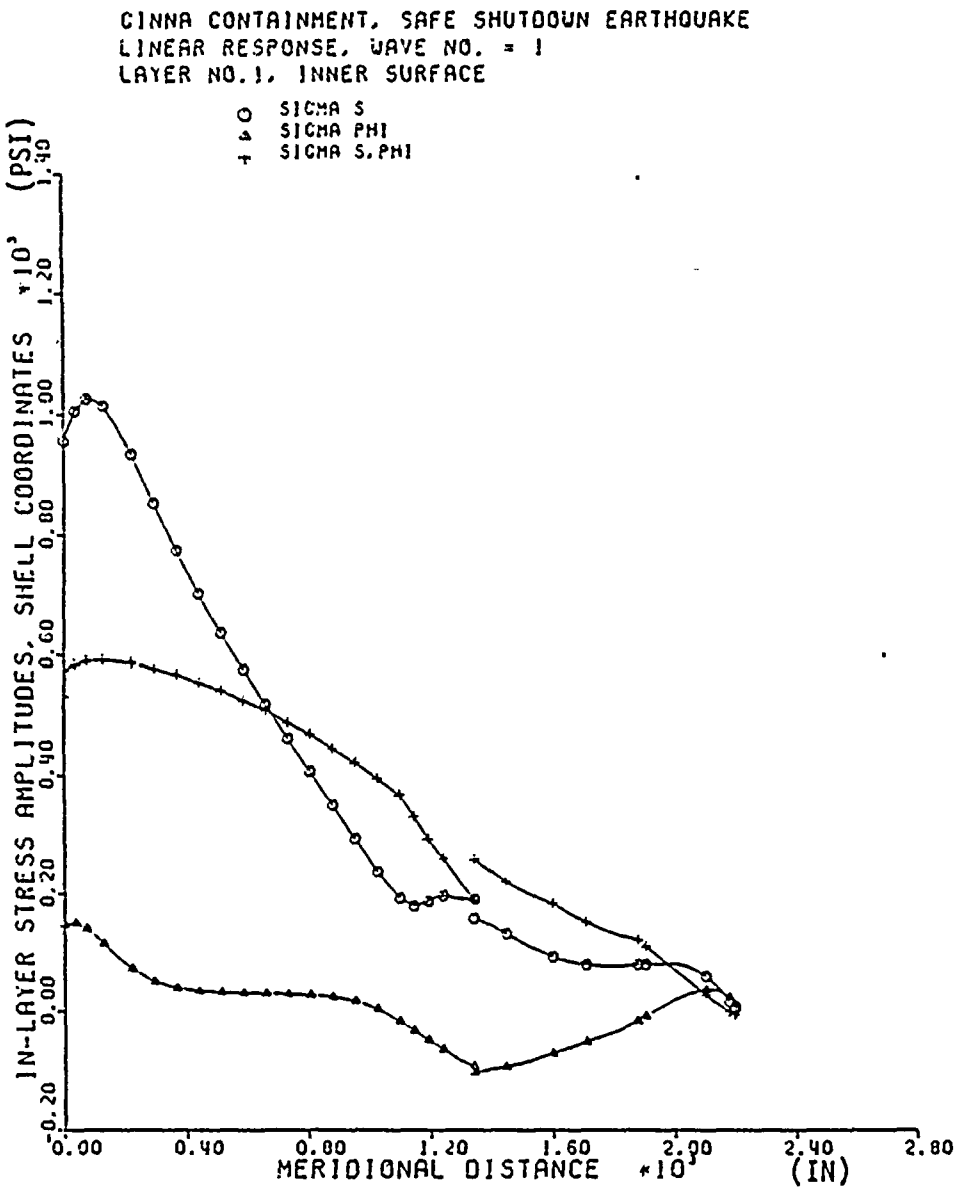

FIGURE 6-1. STEEL LINER MERIDIONAL (S) AND CIRCUMFERENTIAL (ϕ) STRESSES FOR SSE

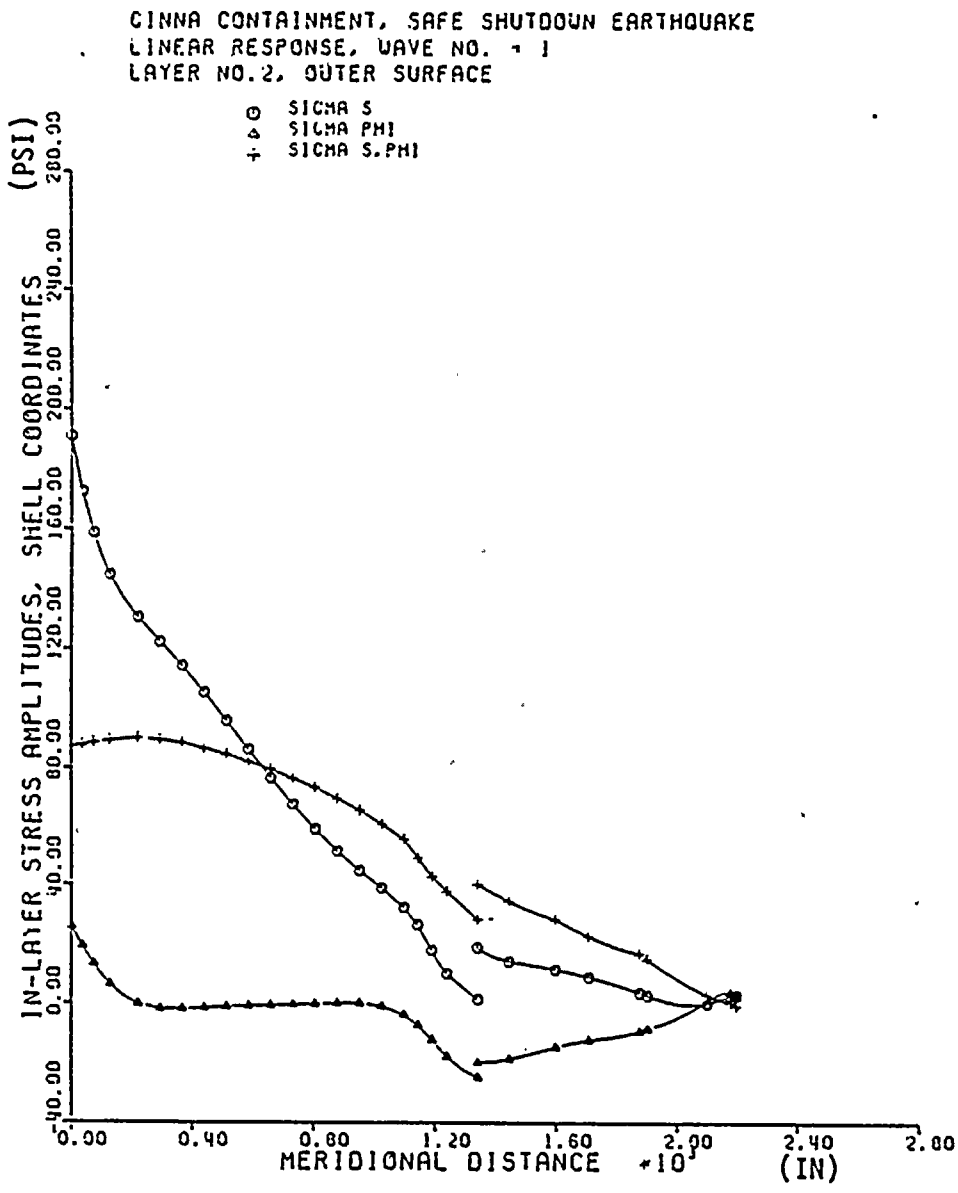

FIGURE 6-2. CONCRETE SHELL MERIDIONAL (S) AND CIRCUMFERENTIAL (ϕ) STRESSES FOR SSE

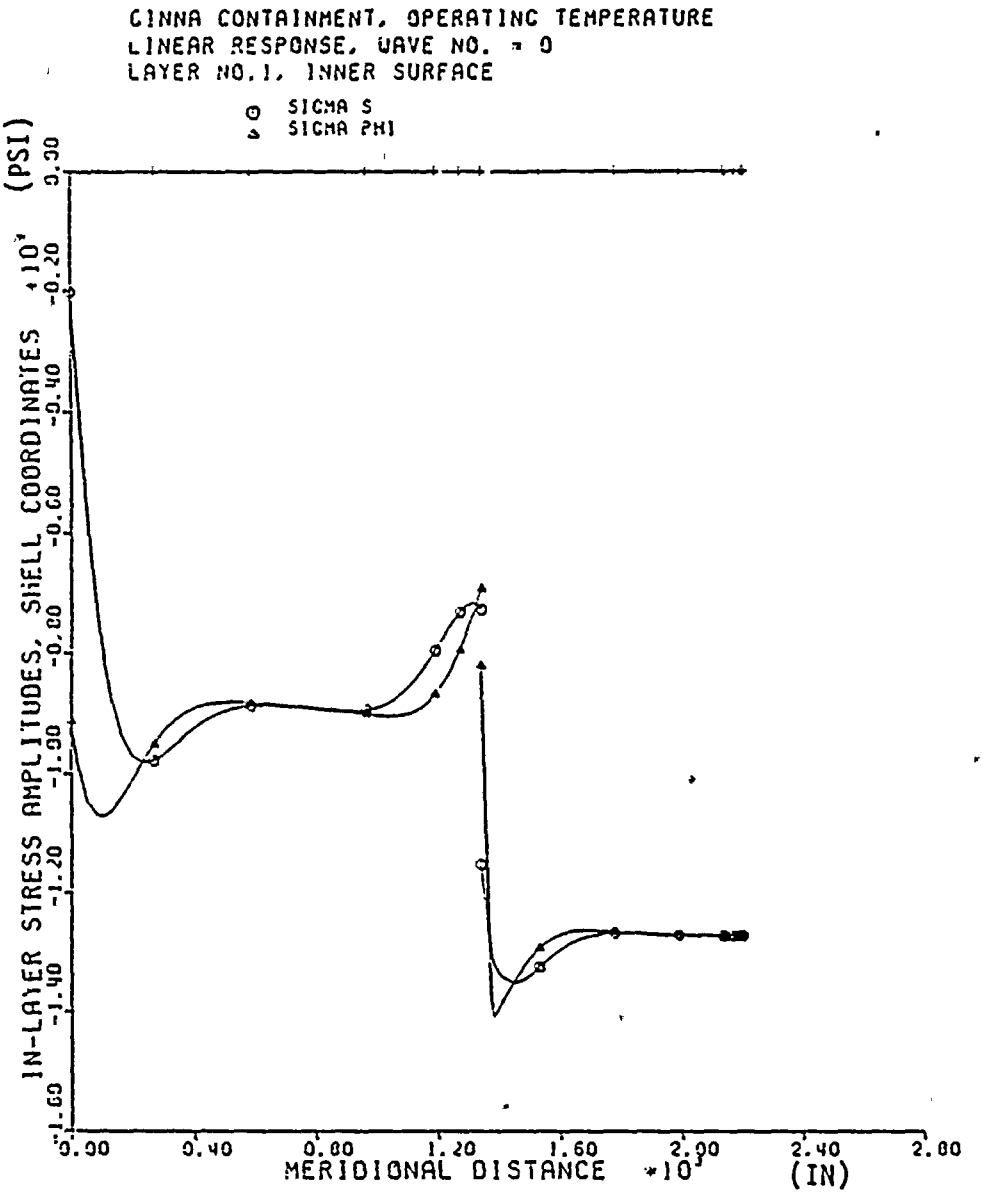

FIGURE 6-3. STEEL LINER MERIDIONAL (S) AND CIRCUMFERENTIAL (ϕ) STRESSES FOR OPERATING TEMPERATURE

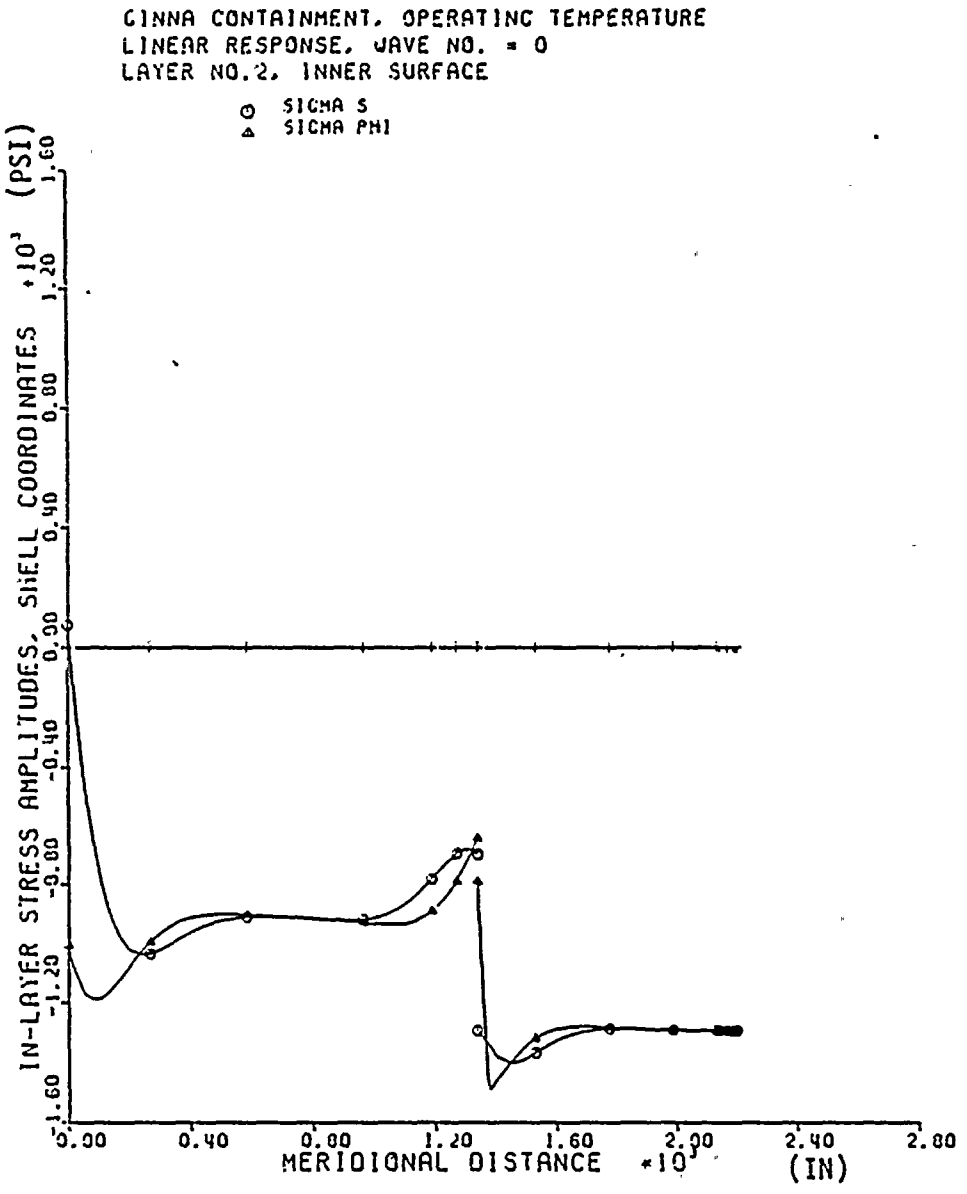

FIGURE 6-4. CONCRETE SHELL INNER SURFACE MERIDIONAL (S) AND CIRCUMFERENTIAL (ϕ) STRESSES FOR OPERATING TEMPERATURE

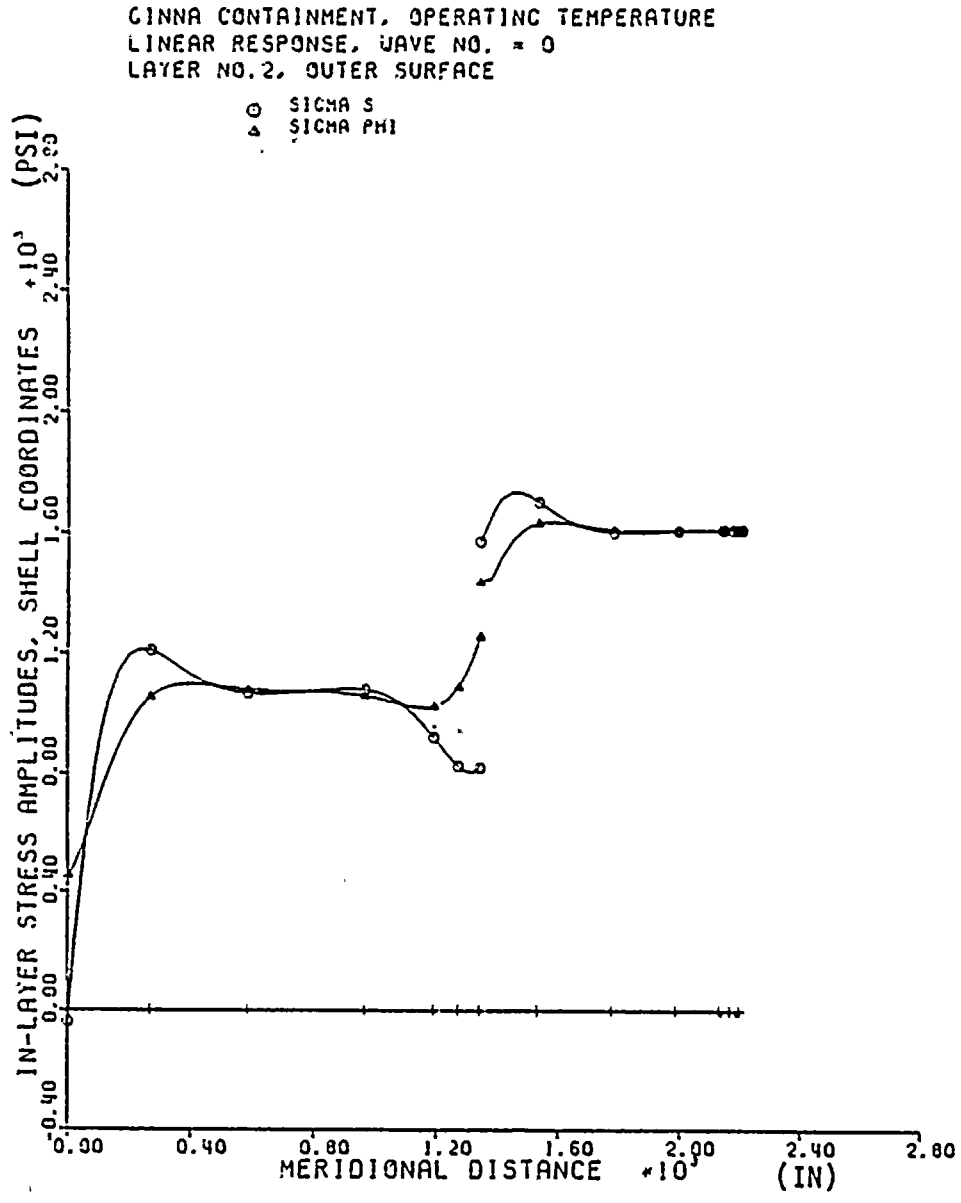

FIGURE 6-5. CONCRETE SHELL OUTER SURFACE MERIDIONAL (S) AND CIRCUMFERENTIAL (ϕ) STRESSES FOR OPERATING TEMPERATURE

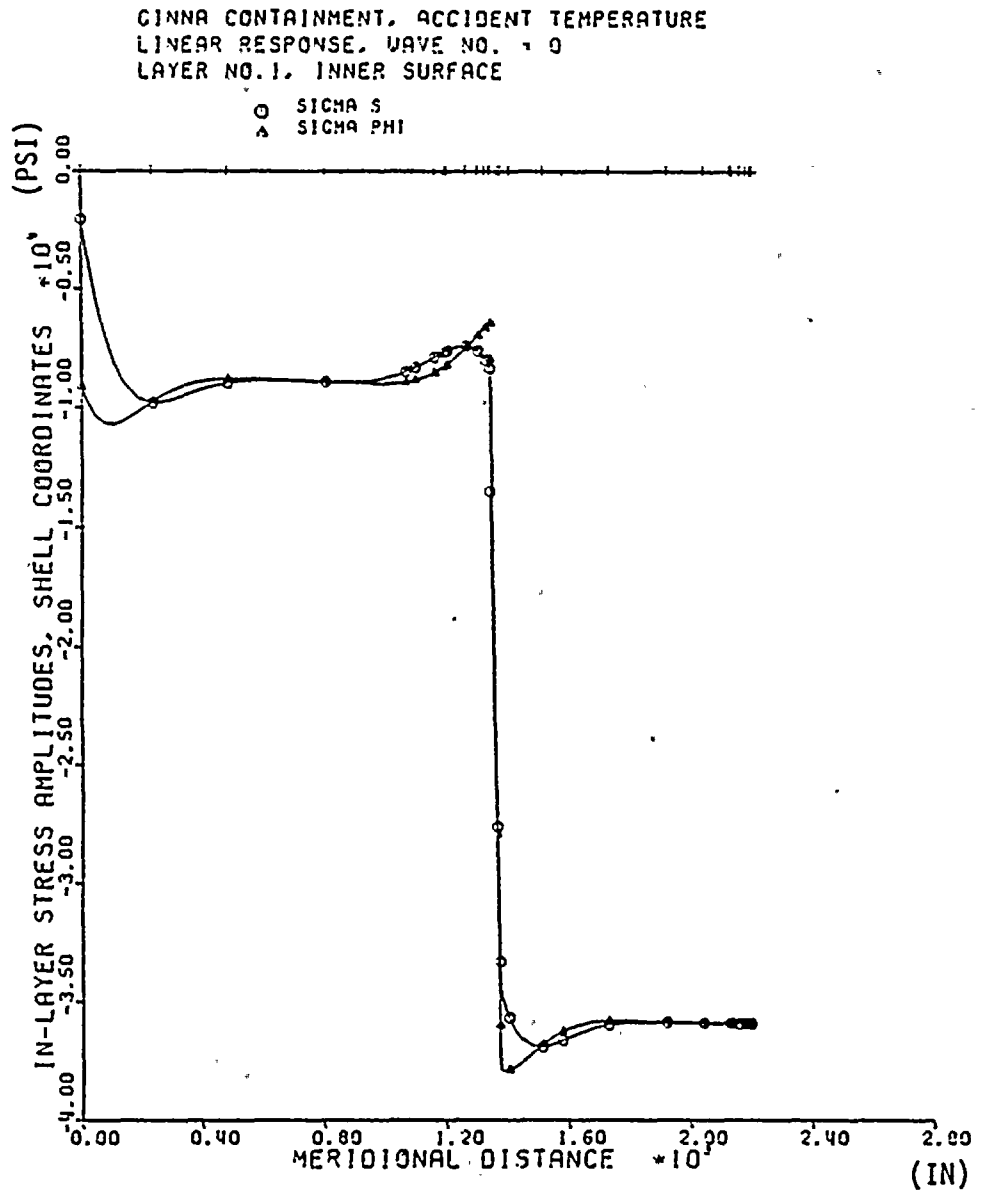

FIGURE 6-6. STEEL LINER MERIDIONAL (S) AND CIRCUMFERENTIAL (ϕ) STRESSES FOR ACCIDENT TEMPERATURE AT T = 94 SECONDS

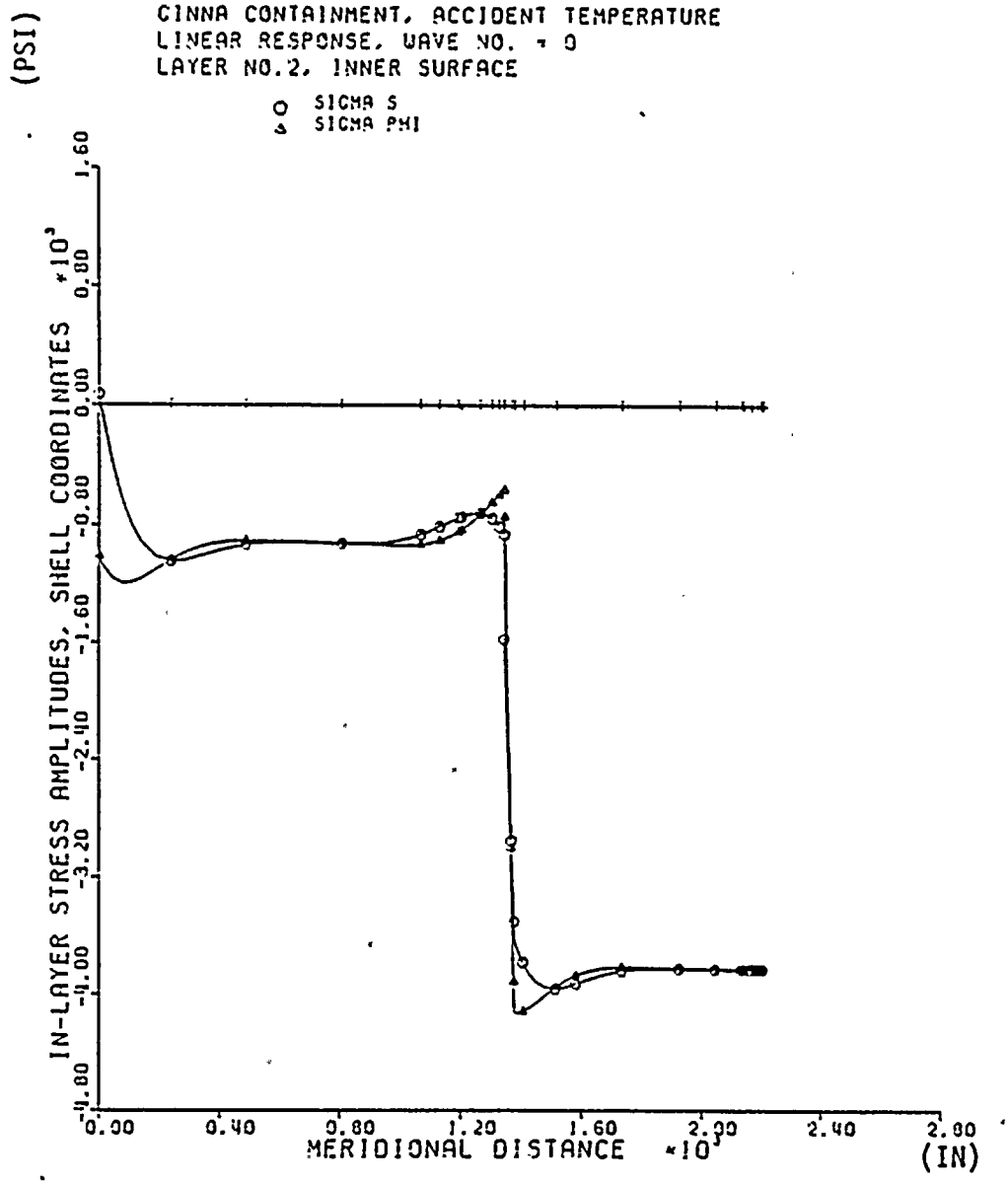

FIGURE 6-7. CONCRETE SHELL INNER SURFACE MERIDIONAL (S) AND CIRCUMFERENTIAL (ϕ) STRESSES FOR ACCIDENT TEMPERATURE AT T = 94 SECONDS

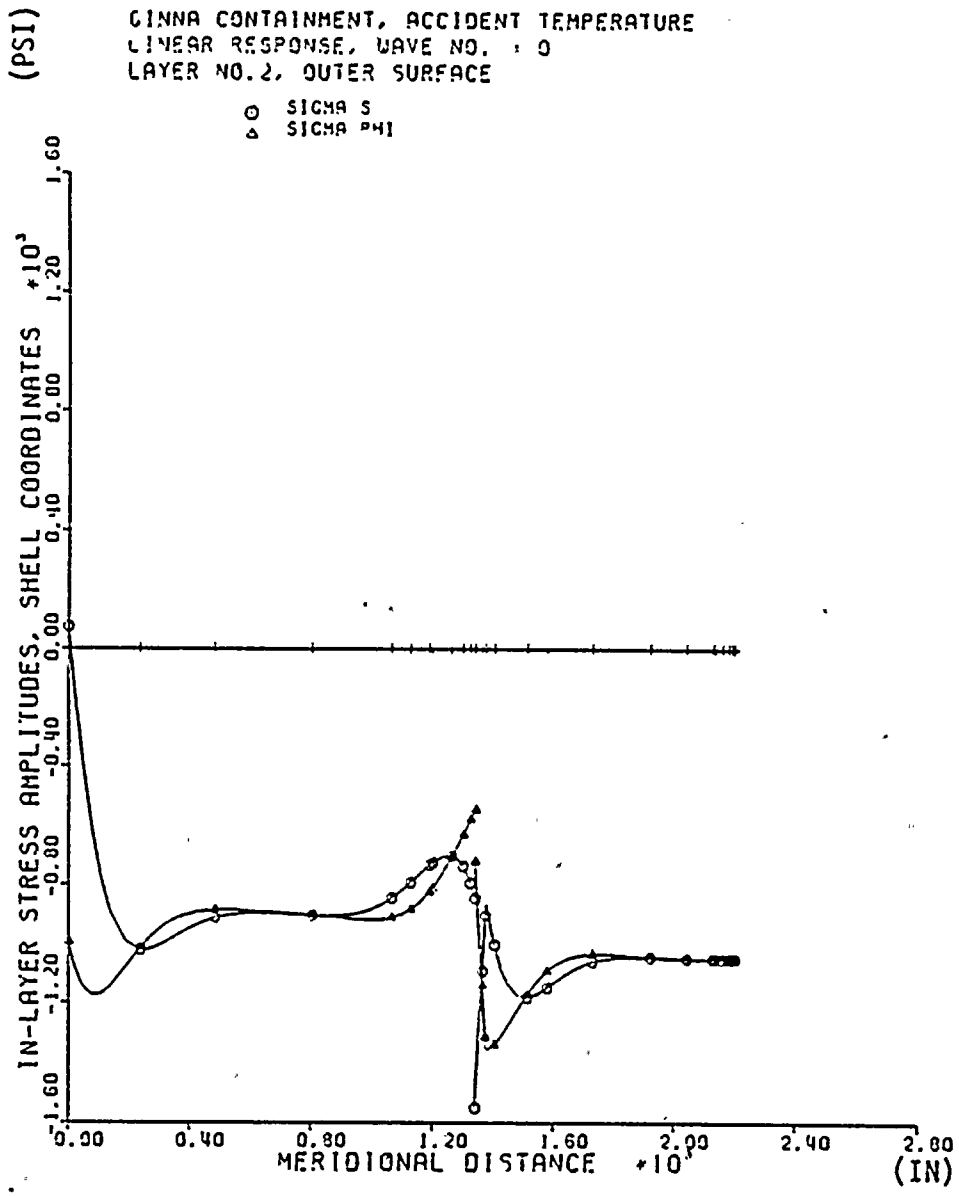

FIGURE 6-8. CONCRETE SHELL MERIDIONAL (S) AND CIRCUMFERENTIAL (ϕ) STRESSES 0.25" FROM INNER SURFACE FOR ACCIDENT TEMPERATURE AT T = 94 SECONDS

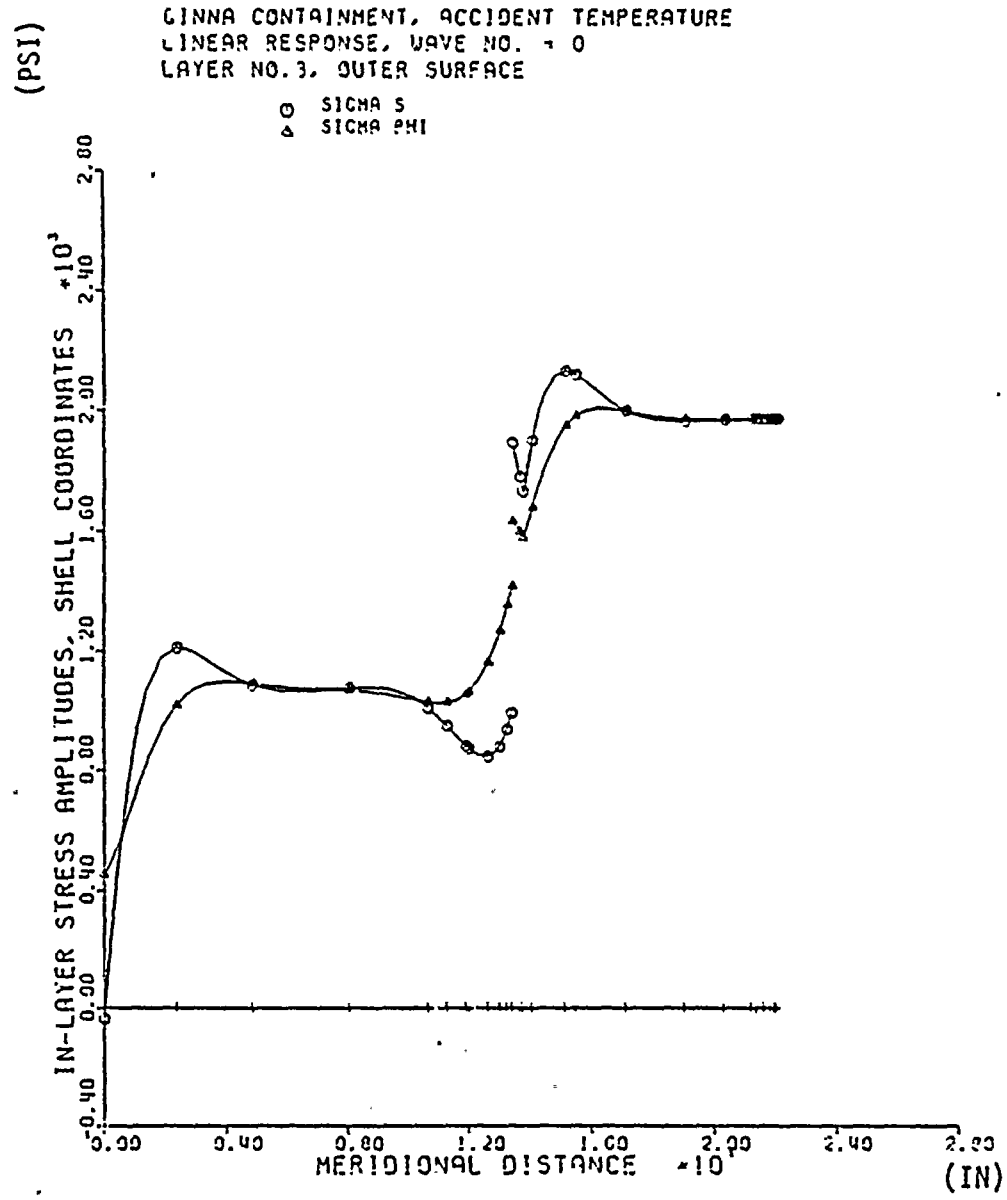

FIGURE 6-9. CONCRETE SHELL OUTER SURFACE MERIDIONAL (S) AND CIRCUMFERENTIAL (ϕ) STRESSES FOR ACCIDENT TEMPERATURE AT T = 94 SECONDS

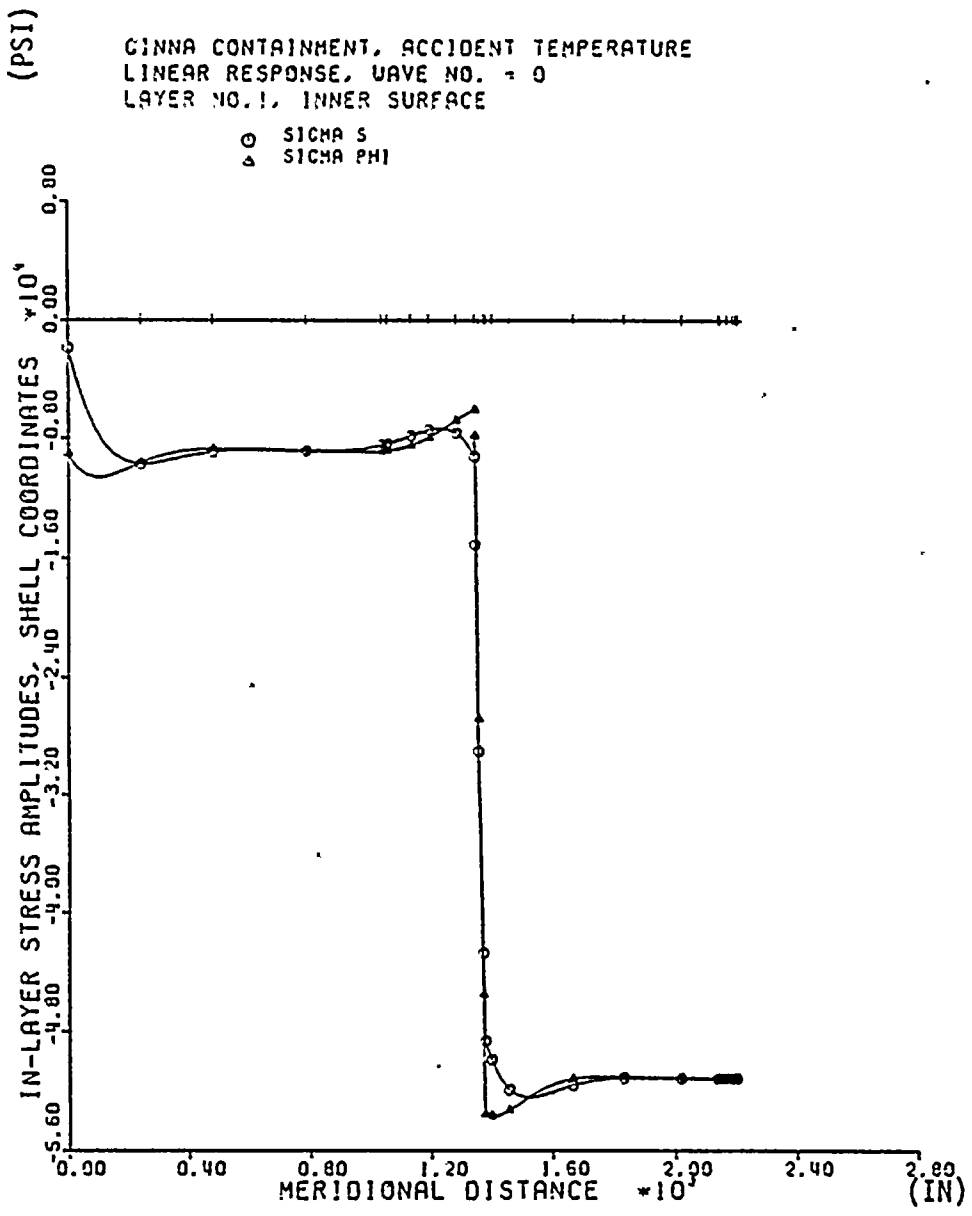

FIGURE 6-10. STEEL LINER MERIDIONAL (S) AND CIRCUMFERENTIAL (ϕ) STRESSES FOR ACCIDENT TEMPERATURE AT T = 380 SECONDS

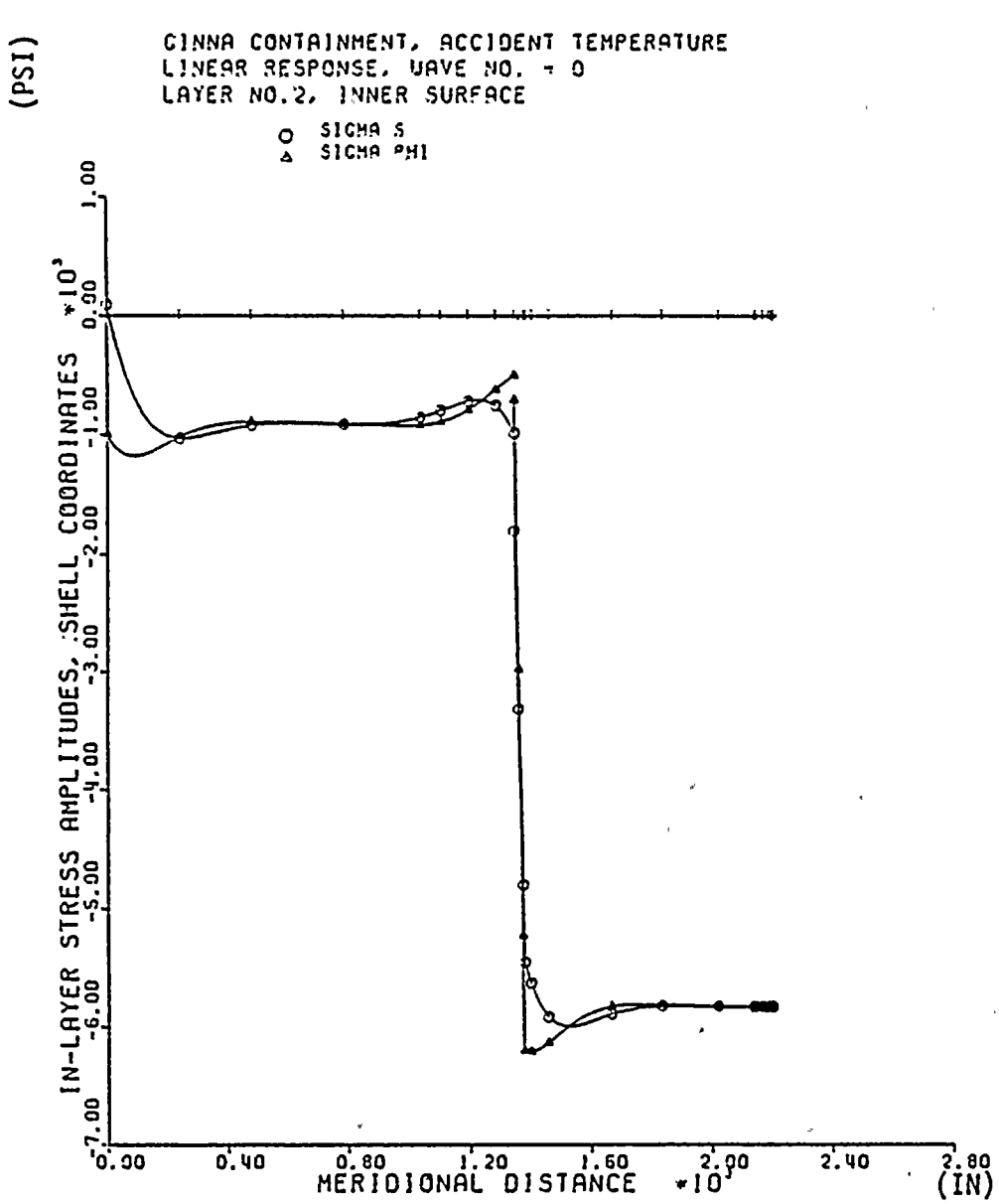

FIGURE 6-11. CONCRETE SHELL INNER SURFACE MERIDIONAL (S) AND CIRCUMFERENTIAL (ϕ) STRESSES FOR ACCIDENT TEMPERATURE AT T = 380 SECONDS

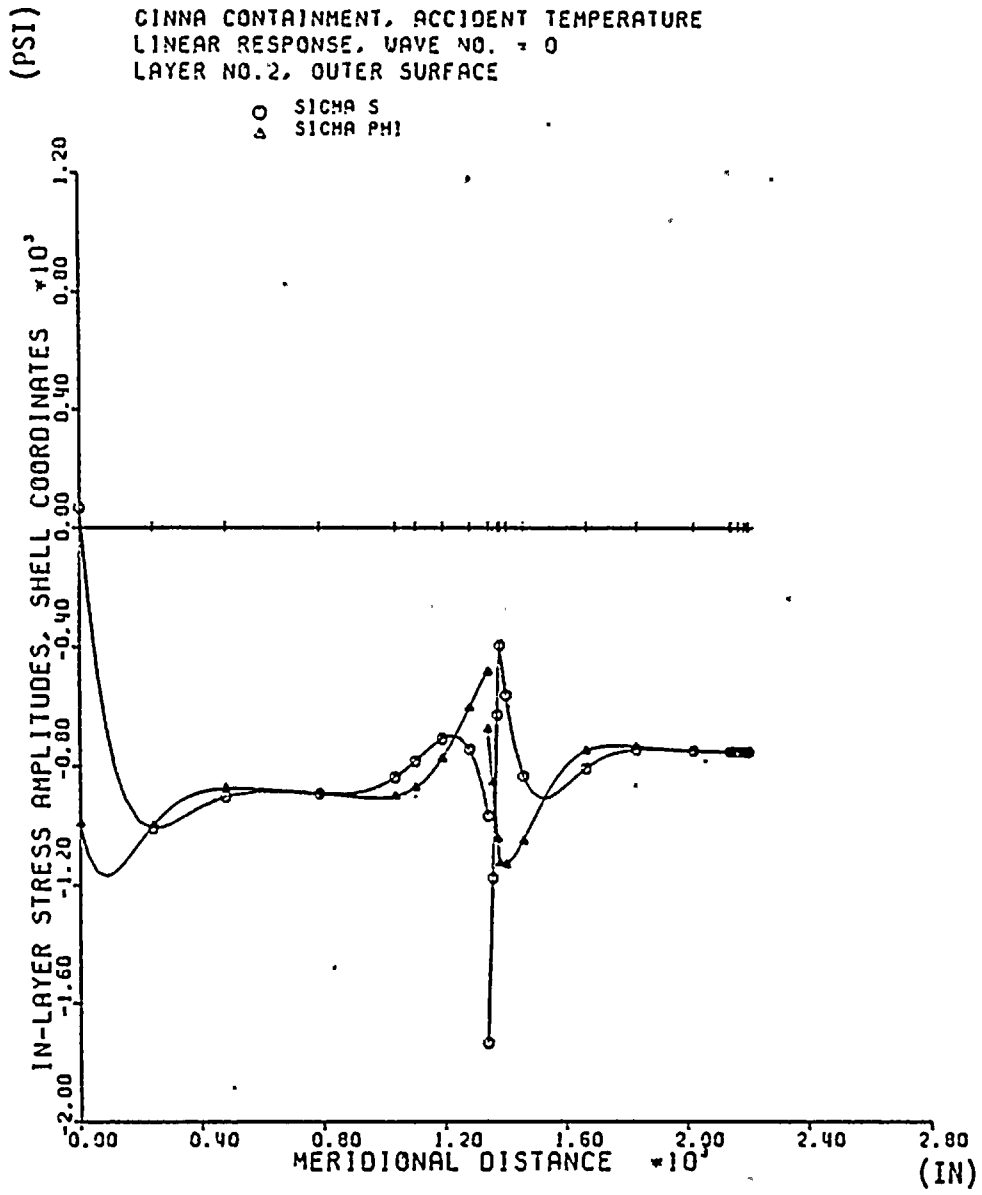

FIGURE 6-12. CONCRETE SHELL MERIDIONAL (S) AND CIRCUMFERENTIAL (ϕ) STRESSES 0.8 INCHES AWAY FROM INNER SURFACE FOR ACCIDENT TEMPERATURE AT T = 380 SECONDS

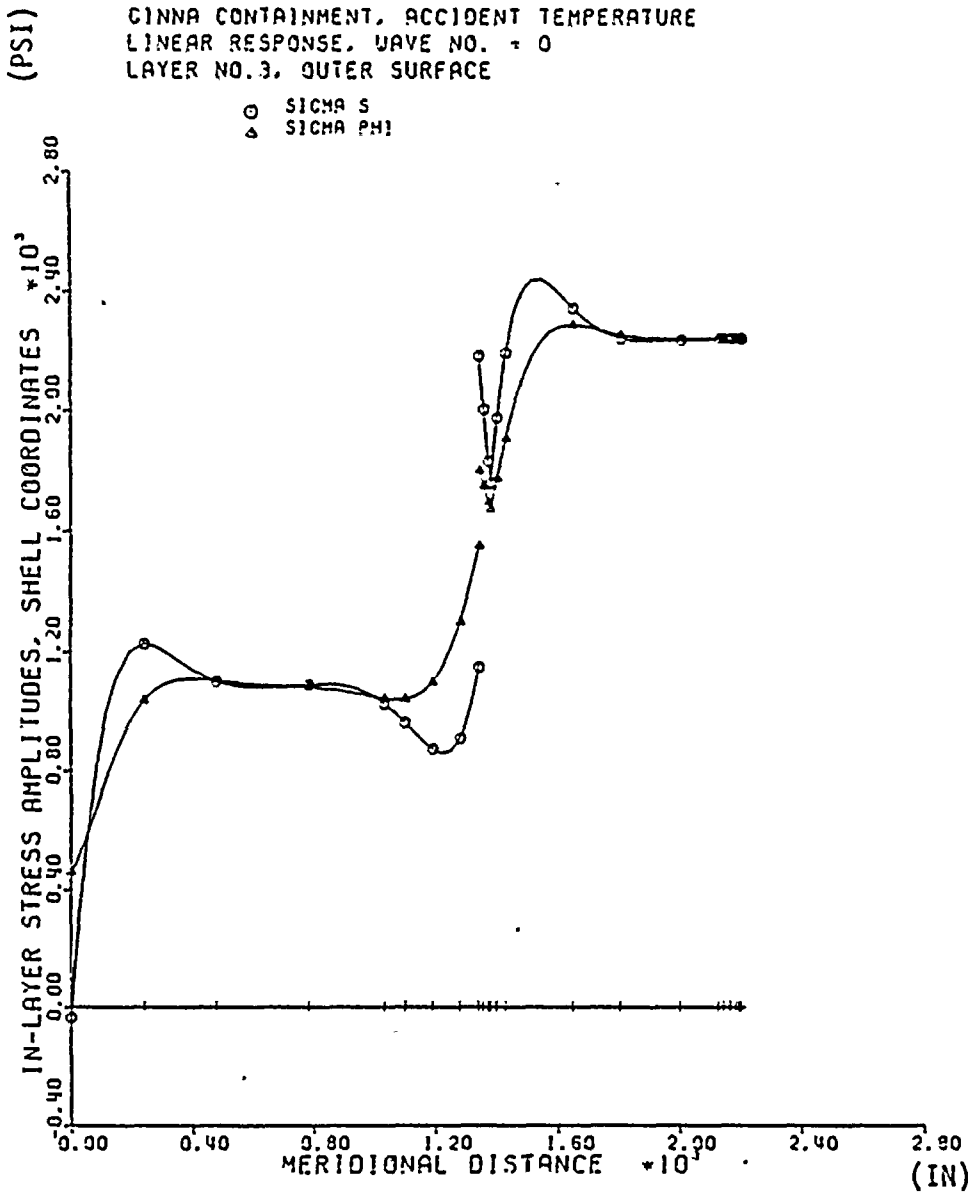

FIGURE 6-13. CONCRETE SHELL OUTER SURFACE MERIDIONAL (S) AND CIRCUMFERENTIAL (ϕ) STRESSES FOR ACCIDENT TEMPERATURE AT T = 380 SECONDS

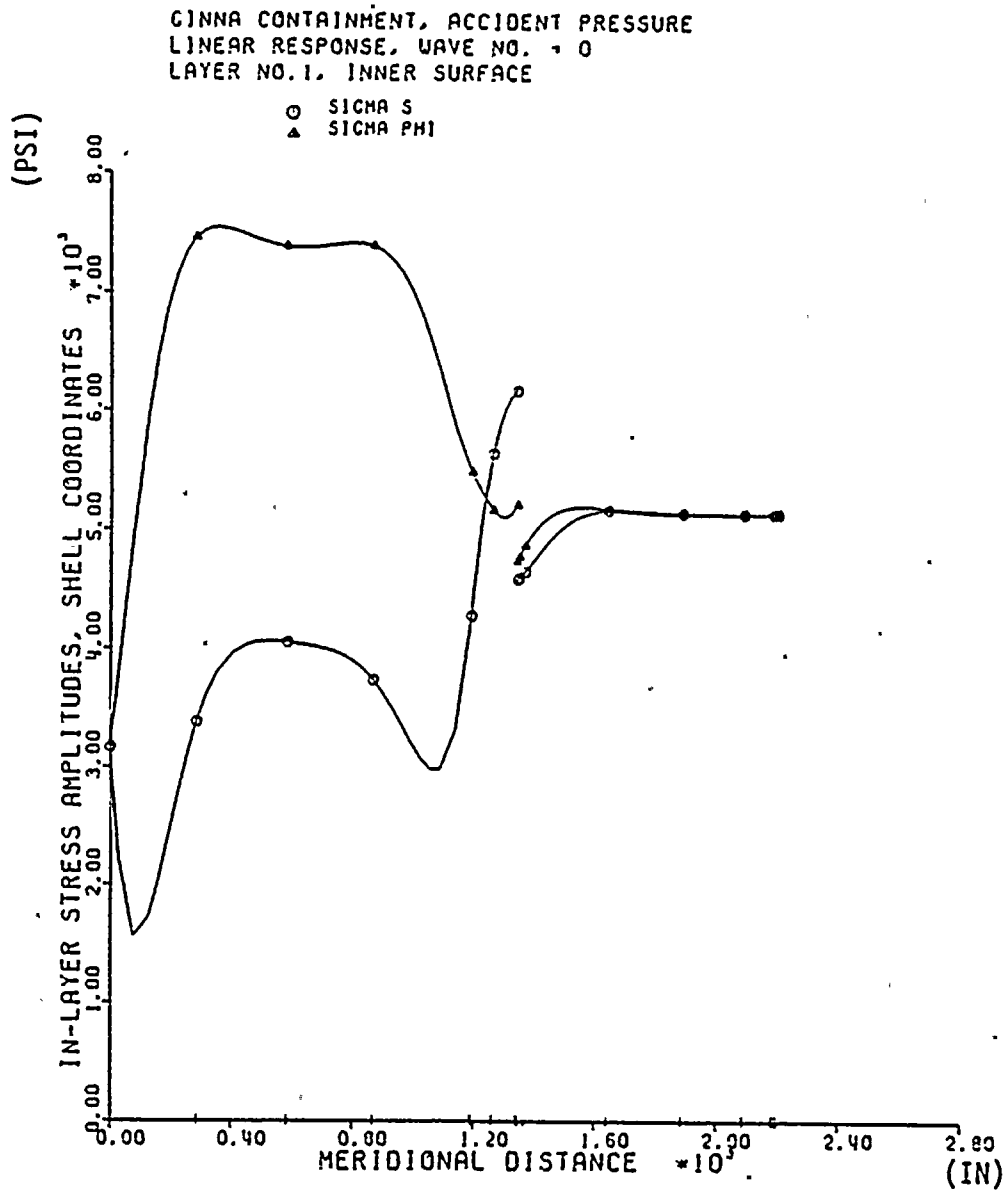

FIGURE 6-14. STEEL LINER MERIDIONAL (S) AND CIRCUMFERENTIAL (ϕ) STRESSES FOR ACCIDENT PRESSURE (P = 86 PSIA) AT T. = 94 SECONDS

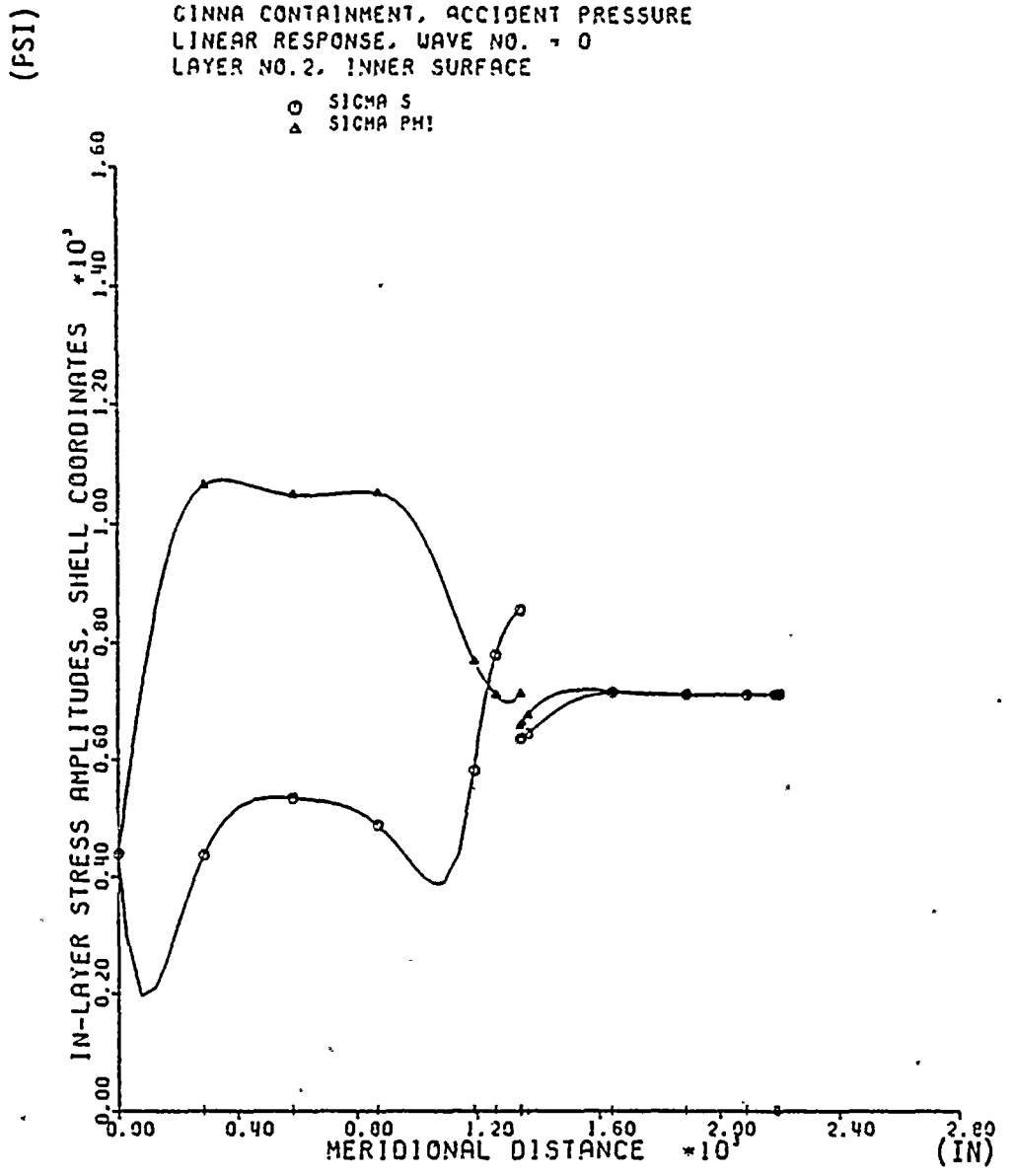

FIGURE 6-15. CONCRETE SHELL MERIDIONAL (S) AND CIRCUMFERENTIAL (ϕ) STRESSES FOR ACCIDENT PRESSURE (P = 86 PSIA) AT T = 94 SECONDS

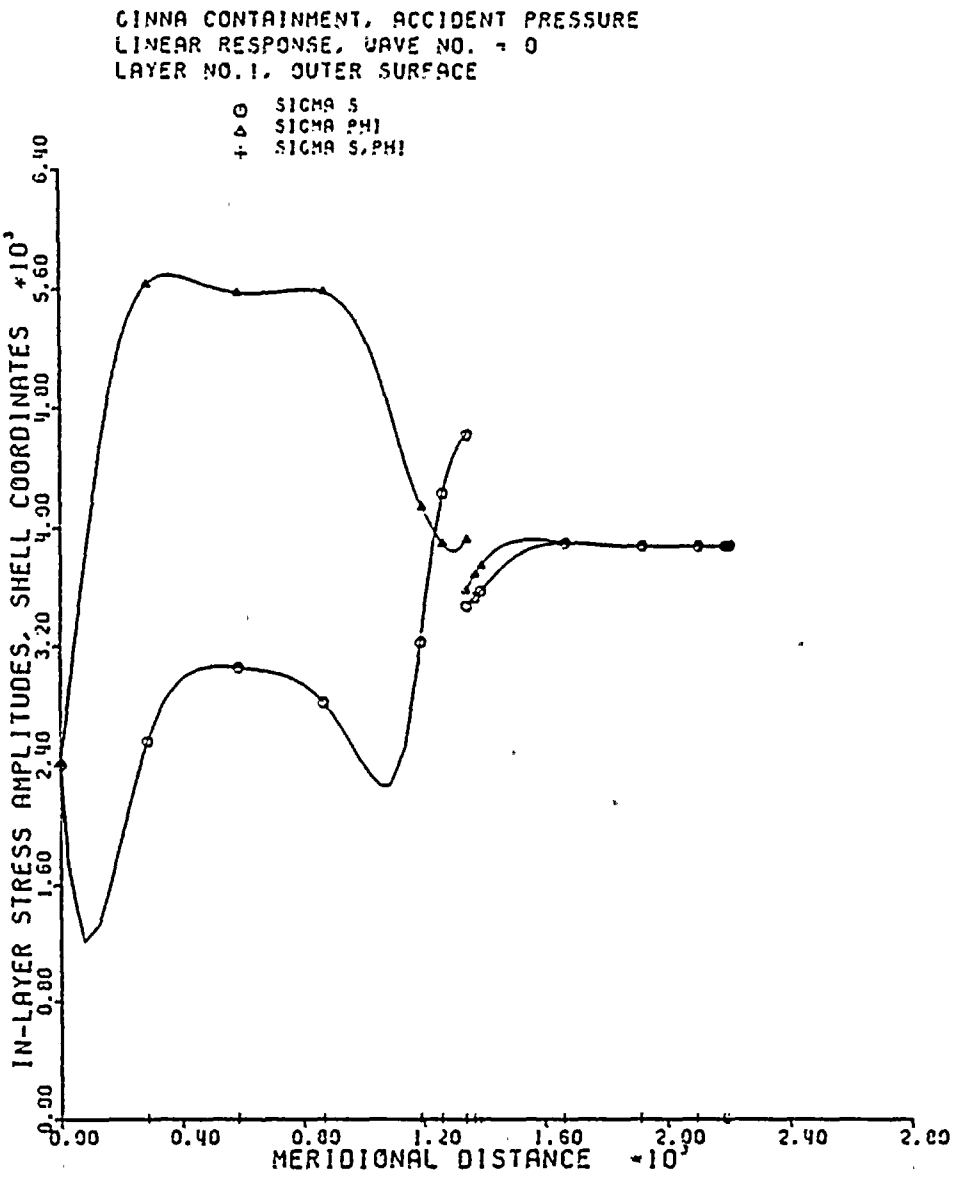

FIGURE 6-16. STEEL LINER MERIDIONAL (S) AND CIRCUMFERENTIAL (ϕ) STRESSES FOR ACCIDENT PRESSURE (P = 69 PSIA) AT TIME = 380 SECONDS

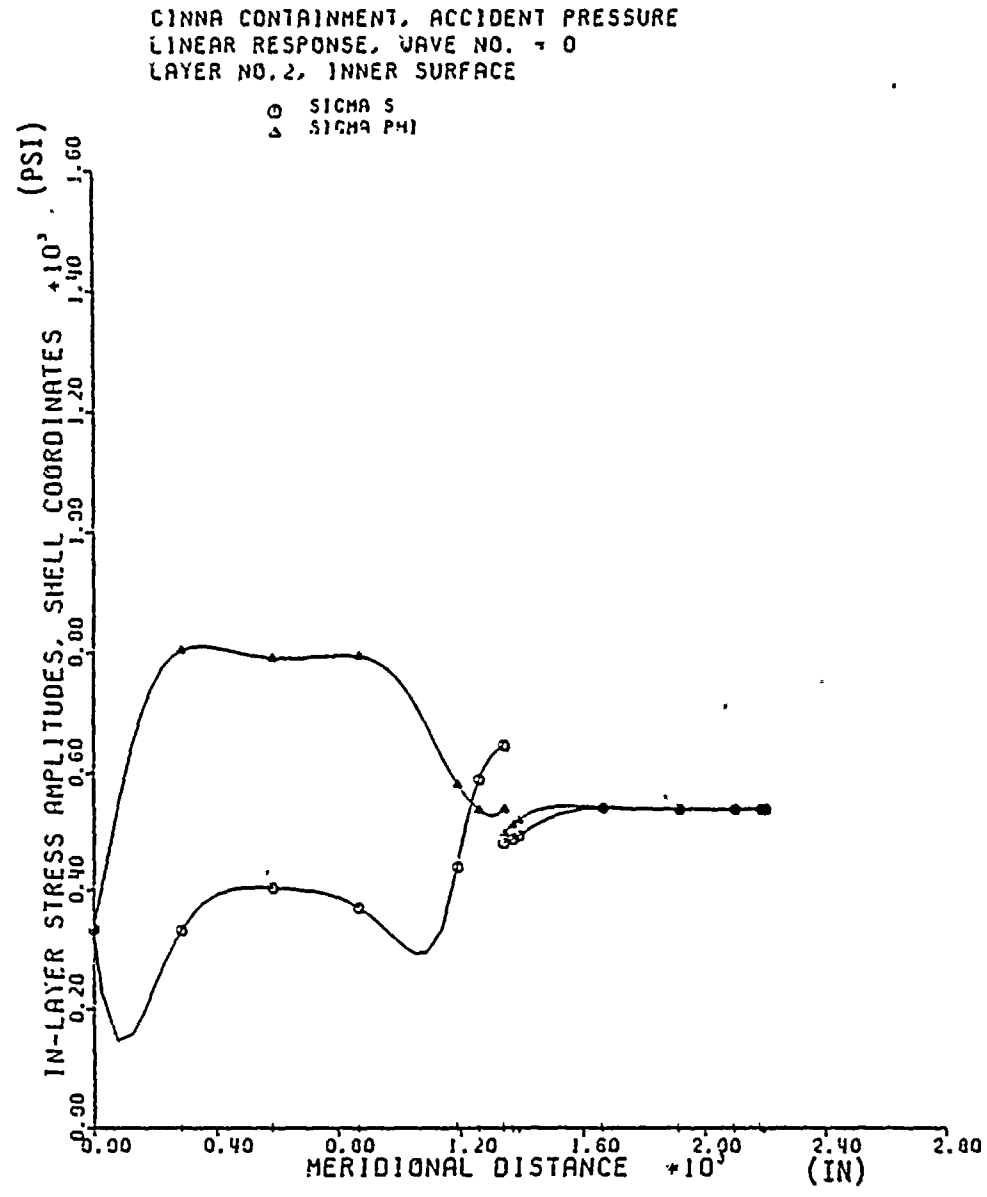

FIGURE 6-17. CONCRETE SHELL MERIDIONAL (S) AND CIRCUMFERENTIAL (ϕ) STRESSES FOR ACCIDENT PRESSURE (P = 69 PSIA) AT T = 380 SECONDS

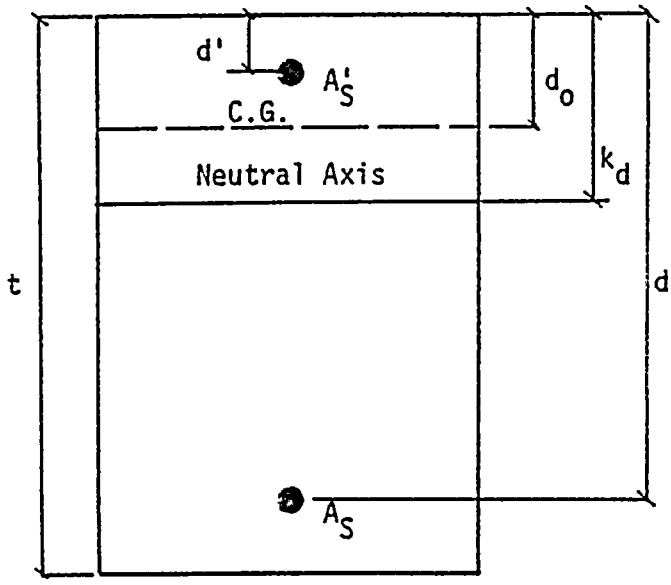

FIGURE 6-18. CRACKED SECTION GEOMETRY

7. LINER BUCKLING

The liner is a 3/8-inch thick Grade 60 steel plate conforming to ASTM 442-60T standards with a minimum yield stress of 32 ksi. The liner anchorage system in the cylinder consists of 3-inch deep channel sections embedded in concrete with studs in between the channel sections. In the dome, the liner anchorage consists of a square grid of studs at 24-inch spacing. As previously discussed, the analysis results showed that the liner stresses are most critical in the dome. Lower liner stresses result in the cylinder due to the presence of the insulation, assuming it remains intact in the event of the LOCA. The liner stresses in the base slab are unaffected due to the 2-foot thick concrete cover.

For the liner anchorage system in the dome, the liner may be conservatively modeled as a rectangular flat plate in biaxial compression. Since the concrete prevents buckling in the outward radial direction, adjacent panels must buckle in the same (radially inward) direction. However, the liner membrane stress can exceed the material yield stress so that plastic hinges may be expected to form. Simply supported edges were selected for the boundary condition for the plate buckling analysis to reflect this condition. Following this assumption, elastic buckling stress in the dome is computed from Reference 8.

$$f_x = 0.5 \quad \frac{\pi^2 E}{3(1 - \mu^2)} \quad (\frac{t}{b})^2 \quad = 25.6 \text{ ksi}$$

where μ is the Poisson's ratio and t/b is the thickness to width ratio ($0.375/12\sqrt{2}$). This is in close agreement with the buckling stress of 26.4 ksi calculated in the original design analysis. From Figures 6-1 through 6-17, the peak liner stress was calculated to be 48.7 ksi which occurs in the dome adjacent to the insulated part of the containment shell. This stress is higher than both the critical buckling stress (f_x) and the code specified minimum yield stress for the steel liner. Although the local buckling of steel liner does not pose any serious

problems, it may be noted that the liner stress in the insulated panels next to the buckled panels drops to 5.8 ksi. The difference between the loads in these adjacent panels must be carried by the shear studs.

In order to determine the shear force per stud, both the post-buckled load in the liner and the meridional thermal gradient in the liner in the vicinity of the edge of the insulation are needed. Accurate analytical determination of these two items requires detailed evaluations which are considered outside the scope of this investigation. However, a preliminary evaluation of liner adequacy was conducted based on the assumption that the post-buckled load in the liner is approximately equal to the critical buckling load, and that the thermal gradient from the exposed liner temperature to the insulated liner temperature occurs over approximately two feet in the meridional direction. These assumptions result in a shear load of approximately 70 k/ft distributed over three shear studs (or 23.3k per stud).

Based on a summary of experimental results for shear stud capacities (References 10 and 11), a median shear capacity of approximately 21.2 k is expected. For design purposes, a capacity reduction (ϕ) factor of 0.85 is recommended, or a capacity of 18 k per stud. Note that Reference 10 recommends a lower value (16.5 k) for design based on $0.9\ A_s f_y$ where A_s is the stud area and f_y is the yield strength of the material. Based on three studs per foot of circumference to carry the thermal loads, the force developed in the liner exceeds the capacity of the shear studs for either the 21.2 k or 18 k values. The expected mode of failure for the studs in shear is tear-out of the concrete rather than shear failure at the weld. Thus, the liner integrity may be expected to have a reasonable probability of being retained for a typical stud failure.

The failed studs are expected to have some residual capacity. However, based on the assumptions noted above together with the conservative thermal analysis conducted, failure of the liner anchorage system may be expected for at least some of the 15 feet below the top of the

insulation down to the embedded channel anchorage system in the cylinder. The post-buckled shape is deformation limited by the thermal conditions and the liner is in compression. Unless there is rupture of the liner due to a stud perforation, rather than the expected concrete cone tear-out mode of failure for the studs, the liner integrity may likely be retained after buckling. This cannot be guaranteed, however, on the basis of the assumptions and analysis described above.

REFERENCES

1. Newmark, N. M. and W. J. Hall, "Development of Criteria for Seismic Review of Selected Nuclear Power Plants," U.S. Nuclear Regulatory Commission, NUREG/CR-0098 (1978).

2. "Rochester Gas and Electric Corporation Robert Emmett Ginna Nuclear Power Plant Unit No. 1 Final Facility Description and Safety Analysis Report," U.S. Nuclear Regulatory Commission, Exhibit D-5 (1968), Volumes 1 and 2, also NRC Docket items 50244-1 and -2.

3. Murray, R. C. et. al., "Seismic Review of the Robert E. Ginna Nuclear Power Plant as Part of the Systematic Evaluation Program," U.S. Nuclear Regulatory Commission, NUREG/CR-1821, UCRL-53014, 1980.

4. Draft Report, "Safety Evaluation Report on Containment Pressure and Heat Removal Capability, SEP Topic VI -3, and Mass and Energy Release for Possible Pipe Break Inside Containment, SEP Topic VI - 2.D, for the R. E. Ginna Nuclear Power Plant", US NRC Docket No. 50-244, 1981.

5. ANSYS Rev. 3, Swanson Analysis Systems, Inc., P.O. Box 65, Houston, Pennsylvania.

6. FASOR - Field Analysis of Shells of Revolution, Structures Research Associates, 465 Forest Ave., Laguna Beach, California.

7. Cohen, G. A., "FASOR - A Program for Stress, Buckling and Vibration of Shells of Revolution", Structures Research Associates, Laguna Beach, California.

8. Data Sheets on Structures, Royal Aeronautical Society, December, 1964.

9. Bleich, F., "Buckling Strength of Metal Structures," McGraw-Hill Book Company, 1952.

10. "Embedment Properties of Heated Studs," TRW Nelson Stud Division, 1977.

11. Ollgaard, J. G., et al "Shear Strength of Stud Connectors in Lightweight and Normal-Weight Concrete", AISC Engineering Journal, April, 1971.

12. ASME Boiler and Pressure Vessel Code, Section III, Division 2, 1980 Edition.